*Graphical Abstract (for review)

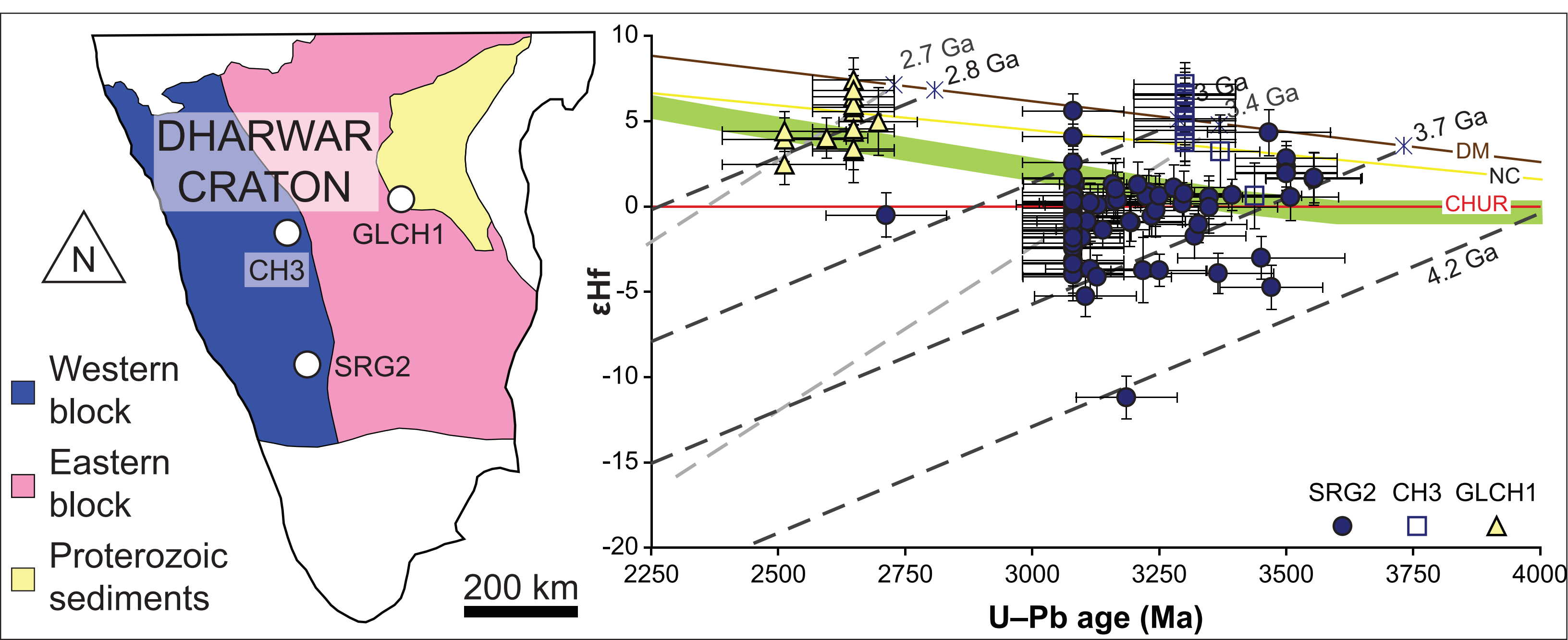

*Manuscript
Click here to view linked References

Contrasting crustal evolution processes in the Dharwar craton: Insights from detrital zircon U–Pb and Hf isotopes

Penelope J. Lancaster[a,*], Sukanta Dey[b], Craig D. Storey[a], Anirban Mitra[b] and Rakesh K. Bhunia[b]

[a]School of Earth and Environmental Sciences, University of Portsmouth, Burnaby Bldg., Burnaby Rd., Portsmouth, PO1 3QL, UK (* penny.lancaster@port.ac.uk; +44 2392 842272)
[b]Department of Applied Geology, Indian School of Mines, Dhanbad, 826004, India

Abstract

New *in situ* U–Pb-Hf analyses of detrital zircons from across the Archaean Dharwar craton indicate significant juvenile crustal extraction events at ~3.3 and 2.7 Ga, and continuous extraction from 3.7–3.3 Ga. Reworking in the older western block at ~3.0 Ga marks the onset of cratonisation, most likely due to 'modern' plate tectonic processes, while reworking in both the western and younger eastern block at 2.55–2.50 Ga indicates accretion of the two terranes and final cratonisation much later than in most other Archaean terranes (~2.7 Ga). Different patterns of disturbance to the zircon U–Pb systematics reflect variations in both the U content of parent rocks and later metamorphic conditions. Tectonic links are observed between the Kaapvaal and western Dharwar cratons, and between the north China and eastern Dharwar cratons, though none of these links necessarily requires a consanguineous origin.

Keywords: Dharwar craton, zircon, U–Pb, Hf model ages, crustal evolution

1. Introduction

Archaean cratons provide a critical window into early Earth dynamics, preserving a record of crustal evolution processes that include the start of 'modern' plate tectonics and the development of supercontinents (e.g., Campbell and Allen, 2008; Næraa et al., 2012). However, these same processes can also destroy or rework substantial volumes of crust, such that only ~7% of the continental crust is older than 2.5 Ga, and the oldest extant Archaean terrane is only ~3.9 Ga (e.g., Hawkesworth et al., 2010; Mojzsis et al., 2014; Shirey and Richardson, 2011). Where Archaean rocks are exposed, bulk techniques such as Pb and Nd isotopes can provide considerable information about continental formation, but these may have been altered by later metamorphic events.

Another method is to examine sedimentary units, which can preserve fragments of the crust that are no longer exposed at the Earth's surface. Resistant detrital minerals such as zircon have particular use in these studies, as they incorporate a range of isotopic and geochemical tracers and can survive multiple crystallisation and/or sedimentary events (e.g., Fedo et al., 2003). Modern *in situ* techniques combined with careful imaging allow direct correlation of crystallisation ages with geochemical information from each growth zone of a mineral, providing context for interpretation even without the parent rock(s). In this manner, a more complete record of a craton's evolution may be obtained, with the benefit of contributions from contrasting isotopic systems.

The Dharwar craton of southern India is one such Archaean block, comprising >2.7 Ga trondjhemite-tonalite-granodiorite (TTG) gneisses, volcano-sedimentary belts (>3.0 and 2.9–2.6 Ga) and 2.7–2.5 Ga calc-alkaline to potassic granitoids (e.g., Chadwick et al., 2007; Jayananda et al., 2000, 2006; Jayananda et al., 2013a; Manikyamba and Kerrich, 2012). These rocks preserve evidence for several cycles of supracrustal formation, deformation, metamorphism and granitic activity during the Precambrian (Table 1). Significant work has been undertaken on these units with bulk techniques, especially εNd, identifying considerable reworking of older crust into younger units (summary in Dey, 2013; Mohan et al., 2013a; Peucat et al., 2013), although very little zircon Hf isotopic work has been published to date (e.g., Mohan et al., 2013b; Santosh et al., 2014; Sarma et al., 2012). However, several important issues remain intensely debated, including the timing and nature of juvenile crust formation and crustal reworking events in the Dharwar craton and how they correlate with events recognised globally, the tectonic context of these events, and differences in the evolutionary histories between the two main blocks of the craton (e.g., Chardon et al., 2011;

Dey, 2013; Jayananda et al., 2013b; Maibam et al., 2011; Manikyamba and Kerrich, 2012; Peucat et al., 2013; Santosh et al., 2014). This study examines zircons from three supracrustal units from different stratigraphic levels as a window into the evolution of the continental crust from a new angle.

2. Geological background

The southern Indian peninsula consists of a northern Archaean domain (Dharwar Craton) and a southern, chiefly Proterozoic, domain (e.g., Bhaskar Rao et al., 2003). The Dharwar Craton is divided in turn into older western (WDC) and younger eastern (EDC) blocks, although a separate central block has also been proposed (e.g., Jayananda et al., 2006; Peucat et al., 2013; Swaminath and Ramakrishnan, 1981). The WDC is dominated by 3.35–3.0 Ga TTG gneisses, most of which report εNd values equal to or less than CHUR, indicating reworking of older crustal material (e.g., Beckinsale et al., 1980; Dey, 2013; Meen et al., 1992). Highly deformed >3.0 Ga Sargur Group greenstone belts are interlayered with the TTG units, and reached peak metamorphic conditions of ~8 kbar and 700–750ºC at ~2430 Ma (Janardhan et al., 1982; Jayananda et al., 2013b; Raith et al., 1983). These belts are in turn unconformably overlain by the younger (2.9–2.6 Ga) Dharwar-type greenstone belts, consisting of metasedimentary and metavolcanic rocks which are divided into the lower Bababudan and upper Chitradurga groups (e.g., Kumar et al., 1996; Swaminath and Ramakrishnan, 1981). Minor ~2.60 Ga potassic granites record final cratonisation in the WDC (Jayananda et al., 2006).

The EDC is dominated by 2.7 Ga Kolar-type greenstone belts and 2.7–2.5 Ga calc-alkaline felsic plutonic and volcanic rocks (e.g., Chardon et al., 2002; Dey et al., 2012; Jayananda et al., 2000, 2013a). The Kolar-type belts are predominantly greenschist to amphibolite facies metabasalts— both plume-related (basalts, komatiites, alkaline basalts) and arc-related (basalts, boninites, Nb-enriched basalt-adakites)—with subordinate felsic volcanic rocks and metasediments (e.g., Balakrishnan et al., 1991; Jayananda et al., 2013a; Manikyamba and Kerrich, 2012; Naqvi et al., 2006). Younger granitoids include gneissic TTGs, syn-tectonic high-Mg diorites or sanukitoids, the atypical 'Closepet-type' granitoid and K-rich leucogranites (e.g., Dey et al., 2003, 2009, 2012; Jayananda et al., 1995, 2000; Moyen et al., 2001, 2003). Older (3.3–3.0 Ga) granitoids and metasediments are now only present as remnants, though old and highly variable Nd model ages and xenocrystic zircon U–Pb ages around the EDC suggest these units were once much more abundant (summary in Dey, 2013; Jayananda et al., 2000; Maibam et al., 2011). Accretion of the EDC onto the WDC at ~2.5 Ga was followed by the formation of widespread platformal basins (1.9–0.6 Ga), including the Cuddapah basin in the far east, which received detritus from the surrounding Archaean basement (Saha and Mazumder, 2012; Saha and Tripathy, 2012).

Structural comparisons between the two blocks provide important clues to late Archaean crustal evolution processes. Chadwick et al. (2000, 2007) argued that the EDC was formed during the Neoarchaean in a convergent setting where oceanic lithosphere was subducted in a WNW direction below a Mesoarchaean foreland continental margin (i.e., the WDC). The Neoarchaean schist belts of the EDC were therefore interpreted as intra-arc basins, whereas those of the WDC (the Dharwar Supergroup) were considered marginal or back-arc basins. Some workers have suggested that the WDC, already cratonised and thickened to a large extent by 2.6 Ga, was deformed moderately by transcurrent shear deformation and shortening at 2.55–2.50 Ga, creating the N–S to NNW trending structural fabric of the Dharwar craton (e.g., Chardon et al., 2011). The EDC, however, evolved in a hot Neoarchaean orogen characterised by magmatic accretion, consistent with the presence of high temperature and low pressure metamorphic assemblages (Jayananda et al., 2012). This block behaved differently due to lateral constrictional flow of viscous lower crust under terminal Neoarchaean convergence (Chardon et al., 2011). These conclusions are supported by geophysical work which has identified a much thicker keel underneath the WDC than the EDC (e.g. Borah et al., 2014; Gupta et al., 2003).

Samples were collected from three stratigraphic levels and both blocks of the Dharwar craton (Fig. 1, Table 1). In the WDC, the presumably Mesoarchaean Sargur belt contains quartzites, metapelites, banded magnetite quartzites, Mn-rich rocks, crystalline limestones, amphibolites and metaultramafic rocks. While upper amphibolite to lower granulite facies metamorphism and multiple episodes of deformation have obliterated the original depositional structures of these supracrustal units, a shallow continental margin basin setting can be envisaged from the rock association (Janardhan, 1994; Swaminath and Ramakrishnan, 1981).

Sample SRG-2 was collected from a fuchsite-bearing quartzite band of the Sargur belt in the type area of the Sargur supracrustals, about 4.5 km SE of Sargur town (76°26'20"E, 11°59'31"N). The rock is dominated by quartz grains with sutured contacts (Fig. 2a), in which often large patchy quartz grains are surrounded by an irregular secondary granular matrix of finer quartz grains. The subparallel arrangement of thin muscovite-rich layers imparts a distinct foliation within the rock, and suggests it was originally a quartz-rich sedimentary rock with a subordinate clay matrix which suffered considerable post-depositional deformation, re-crystallisation and sub-grain formation. Deposition can be constrained to between ~3.4 and 3.1 Ga based on whole-rock Sm–Nd isochron ages of 3125±120 Ma and 3352±110 Ma from related mafic-ultramafic units, and a U-Th–Pb chemical age of 3082±66 Ma for monazite from near the western margin of the Chitradurga belt, interpreted as the age of metamorphism of the Sargur Group (Hokada et al., 2013; Jayananda et al., 2008; Mukherjee et al., 2012).

Sample CH3 was collected about 6 km north of Janakal village (76°19'09"E, 13°57'51"N) from a quartzite band at the western margin of the Chitradurga greenstone belt (WDC). This area exposes northwest-trending mature clastic sediments, including quartz arenites and quartz-pebble conglomerates, intercalated with metabasalt bands belonging to the lower part of the Bababudan Group of the Dharwar Supergroup (Geological Survey of India, 2006; Hokada et al., 2013). They are metamorphosed to the upper greenschist to lower amphibolite facies. Sedimentological studies of the mature lower Bababudan conglomerates and arenites implied deposition in a braided fluvial plains developed over a stable gneiss-granite basement (Srinivasan and Ojakangas, 1986). The basement underlying the Chitradurga greenstone belt consists of 3.35–3.0 Ga TTG gneisses and >3 Ga supracrustal rocks of the Sargur belt, while overlying mafic volcanic rocks reported a whole-rock Sm–Nd isochron age of 2.911±0.049 Ga (e.g. Hokada et al., 2013; Jayananda et al., 2008; Kumar et al., 1996; Peucat et al., 1993). Sample CH3 comprises mainly coarse to very coarse sand-sized grains of mono- and poly-crystalline quartz, surrounded by smaller quartz grains (Fig. 2b). Subordinate thin muscovite flakes are arranged in thin subparallel layers defining a foliation, which in places swerve around the larger quartz grains. It is evident that the rock has suffered deformation and recrystallisation forming a tight interlocking mosaic of grains with sutured contacts.

Sample GLCH-1 is a very coarse-grained sandstone collected about 4.5 km east of Dorigallu village (78°04'51"E, 14°25'20"N), along the south-western margin of the Proterozoic pericratonic Cuddapah basin (EDC). The sample belongs to the lower part of the Gulcheru Quartzite Formation, which consists of unmetamorphosed, subhorizontal beds of conglomerates, sandstones and shales deposited in a basin-margin fluvio-aeolian environment (Basu et al., 2014). This formation, the lowermost unit of the Cuddapah Supergroup, unconformably overlies 2.7–2.5 Ga basement granitoids and greenstone belts, which contain minor Palaeoproterozoic granites, syenites and mafic dykes that limit the maximum age of the Gulcheru Formation to around 2.1 Ga (e.g. Chardon et al., 2002; Chardon et al., 2011; Dey et al., 2014b; French and Heaman, 2010; Jayananda et al., 2013a; Kumar et al., 2012; Suresh et al., 2010). A mafic sill intruding the lower part of the Cuddapah Supergroup was dated to between 1.8–1.9 Ga (Anand et al., 2003; Bhaskar Rao et al., 1995; French et al., 2008), implying that initial sedimentation in the Cuddapah basin started at around 1.9–2.0 Ga. Framework grains, commonly surrounded by dark Fe-oxide rims, form a bimodal size distribution within a fine-grained sericitic matrix (~10% of the rock). These framework minerals consist of large 2500–500 μm rounded to subrounded grains of polycrystalline and monocrystalline quartz with subordinate quartzite, chert and highly altered feldspar, and interstitial fine sand-sized grains of subangular to subrounded quartz with minor chert and altered feldspar (Fig. 2c).

3. Analytical methods

Zircons were separated from ~10 kg of samples at the Indian School of Mines by crushing in a mortar and pestle and collecting the 375–75 μm fraction using disposable nylon mesh. Further processing by Mozley Table, heavy liquids (bromoform and methylene iodide) and handpicking yielded a clean zircon cut. Grains were then cast into epoxy mounts, polished to half height and photographed by cathodoluminescence (CL) imaging on a JEOL JSM-6060 LV scanning electron microscope, all at the University of Portsmouth. All grains were examined to identify growth zoning and contaminating features such as cracks and inclusions. Typical CL images are presented in Fig. 3, and all data are presented in Supplementary Table 1.

U–Pb ages were measured by laser ablation quadropole mass spectrometry (LA-Q-ICP-MS) at the University of Portsmouth after Jeffries et al. (2003), using an Agilent 7500cs coupled to a New Wave Research UP-213 Nd:YAG laser. A 30 μm spot was rastered along a 45–60 μm line. Grains were analysed using the ribbon method to avoid an analytical bias towards 'nice' grains (e.g. Mange and Maurer, 1992). The amount of ^{204}Pb in these analyses was below the detection limit, and no common Pb correction was undertaken. Ratios were calculated using an in-house spreadsheet based on LamTool (Košler et al., 2008), measuring GJ-1 as the primary standard and Plešovice as the secondary; all uncertainties were propagated in quadrature. Average ^{206}Pb/^{238}U and ^{207}Pb/^{206}Pb ratios of GJ-1 were 0.09761±0.00178 and 0.06012±0.00206 (n=188, 2SD), respectively, and of Plešovice 0.05432±0.00142 (n=38, 95%) and 0.05321±0.00191 (n=38, 2SD), consistent with published references (Jackson et al., 2004; Sláma et al., 2008). Previous work under the same conditions, using 91500 as the secondary standard before it was polished away, yielded ^{206}Pb/^{238}U and ^{207}Pb/^{206}Pb ratios of 0.17642±0.00395 and 0.07465±0.00243 (n=37, 2SD), respectively. The resulting average ^{207}Pb/^{206}Pb age of 1059±97 Ma (n=37, 2SD) provides confidence that using such a young primary standard yields correct ^{207}Pb/^{206}Pb ages on Archaean samples, albeit with large uncertainties. Only ages from a single growth zone and avoiding irregular features such as cracks and inclusions were used; concordant ages are those with less than 10% difference between their ^{207}Pb/^{206}Pb and ^{206}Pb/^{238}U ages. Concordia plots and discordant arrays were calculated using Isoplot 3.07 (Ludwig, 2003).

U, Pb and Th concentrations were calculated for each analysis using the average values for GJ-1 given in Jackson et al. (2004). Concentrations in Plešovice from this study averaged 361±86, 18±4 and 42±20 (n=37, 2SD), respectively, approximately half the mean provided for pristine grains but consistent with the minimum observed values for pristine material. Both GJ-1 and Plešovice have highly variable 'accepted' concentrations, but previous work using 91500 as a secondary standard against GJ-1 yielded concentrations of 112±30, 20±6 and 40±14, slightly higher but within uncertainty of published values

(Wiedenbeck et al., 2004). The range of concentrations observed in the Dharwar zircons greatly exceeds these uncertainties, suggesting that while the absolute values should be interpreted with caution, the patterns observed across each sample are sound.

Hafnium isotope ratios were measured by LA-MC-ICP-MS at University College Dublin, following Hawkesworth and Kemp (2006). Every separated grain with growth zoning of sufficient size and a U–Pb age <10% discordant was analysed, using 40 µm spots directly over the U–Pb tracks. JMC-475 averaged $^{176}Hf/^{177}Hf$=0.282144±0.00004 (2SD), yielding a correction of +0.000016, while regular analyses of Mud Tank zircon (Yb/Hf ~0.001) produced a JMC-corrected $^{176}Hf/^{177}Hf$ ratio of 0.2825043±0.000025 (n=115, 2SD). An exponential $^{173}Yb/^{171}Yb$ mass bias correction was applied using an in-house spreadsheet. Analyses of the Temora-2 standard zircon (Yb/Hf ~0.07) produced a JMC-corrected $^{176}Hf/^{177}Hf$ ratio of 0.282677±0.000019 (n=12, 2SD), consistent with the published value of 0.282680±0.000024 (2SD; Woodhead et al., 2004). To further test the reliability of this correction over the range of Yb/Hf observed in this study, a synthetic 'zircon' solution of 200 ppb JMC-475 and 0.5 ppb natural Lu was doped with a natural Yb standard. No effect was observed up to a Yb/Hf of ~0.06 ($^{176}Lu/^{177}Hf$ =0.282144±0.0009, 2SD), while concentrations up to a Yb/Hf of ~0.33 reported slightly lower corrected $^{176}Lu/^{177}Hf$ ratios (0.282136±0.00014, 2SD), though still within uncertainty of undoped JMC-475.

εHf values were calculated based on a two-stage model, using the bulk Earth (chondrite uniform reservoir; CHUR) $^{176}Hf/^{177}Hf$ and $^{176}Lu/^{177}Hf$ from Bouvier et al. (2008), depleted mantle (DM) $^{176}Hf/^{177}Hf$ and $^{176}Lu/^{177}Hf$ from Griffin et al. (2002), and the Lu decay constant from Söderlund et al. (2004). The slight lowering observed for high Yb analyses translates into a +0.2 εHf unit shift at 3 Ga, which is insignificant compared to a typical 2σ precision of 1.2 εHf units. Model ages were calculated assuming an average crustal $^{176}Lu/^{177}Hf$ value of 0.015 (Griffin et al., 2002). If the value of Chauvel et al. (2014) is used instead, individual model ages decrease by <100 Ma, on the same order as the 2σ precision on individual U–Pb ages, but the overall conclusions do not change.

4. Results

The two samples from the WDC (SRG-2 and CH3) present quite different age ranges and Concordia distributions. Th older SRG-2 sample yielded 93 valid analyses, nearly all of which are concordant, but form a continuous smear along Concordia from *c*. 3600 to 2750 Ma (Fig. 4a). While it is possible each age records a unique event within this interval, the typically homogeneous and unzoned appearance in CL (Fig. 3) and very high correlation coefficients (ρ) are more consistent with disturbance during later high grade metamorphism (e.g., Halpin et al., 2012; Whitehouse and Kemp, 2010). Concordia is comparatively flat in the Archaean due to the longer half life of ^{238}U, so ancient Pb loss typically drags analyses along the curve, making it much less apparent. In these cases, additional evidence for or against resetting may come from comparing the U–Pb ages to a more resilient isotopic system, such as Hf isotopes, which are discussed later.

In the younger CH3 sample (n=33), nearly half (n=16) are concordant, with the remaining ages plotting along an apparent discordant array or scattering to older discordant ages (Fig. 4b). These older ages indicate at least two more source areas/rocks were contributing to the detritus in this sample; however, constraining the older source(s) is impossible without any clear pattern to these ages. Arranging the data younger than 3.3 Ga in order of decreasing $^{207}Pb/^{235}U$, and alternately rejecting the highest and lowest analyses until a minimum MSWD is reached, yields a line with intercepts at 527 ± 420 and 3284 ± 92 Ma (n=13, MSWD=8.3). The lower intercept age may indicate resetting during the Pan-African event (~550 Ma; Brandt et al., 2014), since half of the analyses which define it contain <100 ppm U (Fig. 5b; e.g., Mezger and Krogstad, 1997), but could also be geologically meaningless.

In the EDC, sample GLCH-1 (n=65) yields slightly fewer concordant ages (n=25; Fig. 4c). Following the same method as for CH3, two discordant arrays between can be calculated between 817 ± 280 and 2647 ± 40 Ma (n=18, MSWD=4.2) and 55 ± 460 and 2511 ± 61 Ma (n=13, MSWD=3.5). The former consists of mostly low U zircons (Fig. 5c), and the lower intercept may correspond to regional magmatism identified in the Southern Granulite Terrane at ~800 Ma (Brandt et al., 2014). The latter contains only two analyses with <100 ppm U, but coincides with terminal crustal reworking and potassic granitic magmatism at 2.52–2.51 Ga (e.g., Dey et al., 2014b; Jayananda et al., 1995, 2013a).

Another method for identifying Pb loss, especially the cryptic loss suspected in SRG-2, is to plot $^{176}Hf/^{177}Hf$ ratios against the measured U–Pb crystallisation ages (Fig. 5). Hf is bound into the zircon structure by direct substitution for Zr, so any change to the Pb systematics will lead to lines of similar $^{176}Hf/^{177}Hf$ ratios over a range of U–Pb ages. These sub-horizontal arrays mimic evolution lines of $^{176}Lu/^{177}Hf=0.005$, as is seen in sample GLCH-1 which displayed clear evidence for Pb loss in Fig. 4c. Two identical lines can be drawn for the data from SRG-2, one through those reporting $^{176}Hf/^{177}Hf$ ratios of ~0.2808 and the other through those of ~0.2806. As such, the analyses falling along these lines are interpreted to have experienced Pb loss similar to that of GLCH-1 and CH3, despite the lack of discordant arrays on a standard Concordia plot.

εHf values have been plotted at both their measured and 'best estimate' U–Pb crystallisation ages (Fig. 7). Against their measured ages, εHf values in both GLCH-1 and CH3 are nearly all positive (0–5), while the majority in SRG-2 are slightly positive to negative (-10–2). These values correspond to extraction ages of 2800–2700 Ma for GLCH-1 and ~3300 Ma for CH3, while individual model ages in SRG-2 fall between 3700 and 3300

Ma. Estimated ages are determined as either the upper intercept of the relevant discordant array (GLCH-1 and CH3) or as the age at which the relevant $^{176}Lu/^{177}Hf$ evolution line intersects the data array clustered along CHUR (SRG-2). These estimated U–Pb ages and the resulting Hf model ages are also presented in the Supplementary data table.

5. Discussion

5.1 Crustal evolution from individual samples

Clear differences are observed both between the WDC and EDC, as well as between the two samples from the WDC, and comparing these data provides greater insight into crustal processes during a critical transitional period in Earth's history (Fig. 7). The two samples from the WDC contain overlapping ranges of U–Pb ages, but mutually exclusive εHf distributions. The older SRG-2 sample contains zircon cores up to 3555 Ma, associated with both oscillatory (magmatic) and unzoned (metamorphic or metamict) patterns in CL images. Similar ages are reported by Nutman et al. (1992), who obtained detrital zircon U–Pb ages from Sargur-type schist belts and concluded that 3.58–3.13 Ga granitoids supplied the detritus. The same authors noted a younger age component of 3.13–2.96 Ga, which they interpreted as the result of high-grade metamorphism due to intrusion of surrounding granitoids.

More negative εHf values correlate with younger U–Pb ages and a transition to overgrowths on existing cores, recording U–Pb ages between 2550–2450 Ma. However, εHf values plot very close to CHUR until ~3000 Ma, before suddenly shifting to negative values and overlapping older zircons in ~2550 Ma greywackes from the Gadag greenstone belt (Sarma et al., 2012). Since older U–Pb ages typically report lower U concentrations (Fig. 5a), younger zircons with higher U concentrations, and hence more radiation damage, were more affected by open system behaviour during later metamorphism (e.g., Kooijman et al., 2011; Mezger and Krogstad, 1997).

The smear of U–Pb ages along Concordia (Fig. 4a) also complicates the determination of Hf model ages for the parent rocks of detritus in SRG-2. Model ages (T_{DM}) for grains reporting U–Pb ages older than ~3000 Ma should be the most reliable, as neither the U–Pb nor Hf systems should have been disturbed. T_{DM} calculated for these grains using the typical upper continental crust $^{176}Lu/^{177}Hf$ of 0.015 range between 3700 and 3500 Ma, with a small number recording model ages up to 4200 Ga. In addition, one zircon core (3466 Ma) plots very close to the DM line, recording a model age of 3500 Ma. Examining the younger grains, which most likely experienced Pb loss, provide an overall model age of ~3400 Ma. Together, these data suggest the Sargur belt was receiving detritus from rocks extracted over ~300 Ma and evolved to zircon-bearing compositions within 400 Ma of extraction, consistent with global averages (e.g., Lancaster et al., 2011).

By contrast, CH3 contains very few concordant U–Pb analyses, all of which report positive εHf values. These zircons overlap the range of U–Pb ages reported elsewhere in the Chitradurga belt and its northern extension, the Gadag belt (e.g., Hokada et al., 2013; Sarma et al., 2012). Very few zircons preserve magmatic zoning in CL, and the youngest concordant magmatic U–Pb age is 3200 Ma. Once again the oldest ages are associated with the lowest U contents (Fig. 5b), while the discordance pattern observed in the U–Pb ages may be due to nanoscale recrystallisation during greenschist facies metamorphism (e.g., Hay and Dempster, 2009b). Apart from a single core dated at 3438 Ma, which plots within the SRG-2 data field and reports a T_{DM} of ~3700 Ma, nearly all the CH3 zircons plot within uncertainty of each other (U–Pb) and the DM (εHf), and report model ages within 300 Ma of crystallisation at ~3200 Ma. Because these data plot so close to the DM, the choice of $^{176}Lu/^{177}Hf$ in the parent rock has little impact on the calculated model age. Together, these observations suggest the detritus in this unit was derived from a single point source, extracted from the mantle ~3300 Ma and reworked to a zircon-bearing composition at ~3200 Ma. Since these zircons record a similar range of U–Pb ages and εHf values as the northern Gadag belt (Sarma et al., 2012), rocks of this description were most likely common within the source area for these supracrustal units.

Sample GLCH-1 reflects the younger rocks found in the EDC. Much like sample CH3, few U–Pb ages are concordant, in this case between 2400 and 2700 Ma, with the rest falling along two very similar discordant arrays (Fig. 4c). Roughly half the analyses were on growth layers with oscillatory zoning in CL, but these analyses were just as likely to be discordant as those with other forms of zoning. The youngest concordant magmatic age, based on oscillatory zoning in CL imaging, is ~2500 Ma, coincident with all concordant metamorphic ages (homogeneous, usually dark, appearance in CL), but does not represent the time of deposition as this basin developed during intracontinental rifting at ~1900 Ma (e.g., French et al., 2008; Saha and Tripathy, 2012). Evidence for exposed Palaeoarchaean material amongst the more abundant Neoarchaean–Palaeoproterozoic basement comes from several sources. Detrital zircons from the younger Owk Shale Fm. (Kurnool Group; Table 1), overlying the Cuddapah Basin sediments and traditionally believed to be Neoproterozoic in age, also record U–Pb ages between 2690 and 2340 Ma, with a single grain at 3300 Ma (Bickford et al., 2013), while remnants of Mesoarchaean granitic gneisses and Palaeoarchaean to Mesoarchaean whole rock Nd depleted mantle model ages and inherited zircons yielded by Neoarchaean granitoids and felsic volcanic rocks of the EDC (Dey, 2013; Dey et al., 2014b; Jayananda et al., 2013a; Mohan et al., 2013a).

Nearly all concordant grains have positive εHf values, which correspond to Hf model ages between 2700 and 3000 Ma. Since nearly all data overlap within uncertainty, though, these most likely derive from a single source with an extraction age between 2700 and 2800

Ma depending on the $^{176}Lu/^{177}Hf$. Whole rock εNd work on basement granitoids and greenstones exposed in the immediate vicinity of GLCH-1 has identified juvenile crustal extraction from 2700–2600 Ma followed by extensive reworking in the EDC from 2580–2520 Ma (Dey et al., 2014b, a; Jayananda et al., 2013a), consistent with the results of GLCH-1. Rocks with similar U–Pb and εHf appears to be common both within and outside the Dharwar craton, as similar zircons are reported in the older Aravalli sediments to the northwest (Kaur et al., 2011, 2013) and felsic volcanic units from southern India (Praveen et al., 2014). Basement anorthosites from the Sittampundi Complex, to the south of the Dharwar craton, also record the same distribution of zircon U–Pb ages, a regional metamorphic event ~715 Ma and εHf values which directly overlap those in this sample (Mohan et al., 2013b).

5.2 Crustal evolution in the wider Dharwar craton

While each detrital sample only records a small part of the craton's evolutionary history, together they provide a more complete picture. Although collected far from each other, the zircons in both SRG-2 and CH3 overlap published data from around the WDC, suggesting they are representative of broader crustal processes in the region. The oldest zircons in SRG-2 form a continuous array around CHUR until ~3000 Ma, suggesting rocks which evolved to zircon-bearing compositions were extracted continuously from the mantle from ~3700 to at least 3400 Ma. In addition, both SRG-2 and CH3 record zircons >3000 Ma with similar U–Pb ages but different εHf values. Together, these observations suggest the WDC contains discrete fragments of crust extracted at different times, in keeping with the model of pre-modern plate tectonics whereby it was similarly easy to make and destroy new crust (e.g., Hawkesworth et al., 2009).

TTG gneisses aged between 3400–3200 Ma are well exposed in the WDC (e.g., Beckinsale et al., 1980; Bhaskar Rao et al., 2008; Meen et al., 1992; Meert et al., 2010;

Peucat et al., 1993). While reworking of older crust is associated with the extraction of juvenile material (e.g., Meen et al., 1992), the preponderance of zircons of these ages reporting εHf >CHUR suggests little mixing between juvenile and pre-existing crust, a conclusion also reflected by εNd data from these units (e.g., Devaraju et al., 2007; Jayananda et al., 2008; Peucat et al., 1993). Regional metamorphism is first noted at ~3100–3000 Ma (Jayananda et al., 2013b), which coincides with both crystallisation in the juvenile source of CH3 and the onset of Pb loss in SRG-2. These oldest zircons report the lowest U contents (typically <100 ppm), but there is no clear cut-off in U concentration between the presence or absence of open system behaviour. While U(-Th-Rb) depletion in whole rocks is linked to sub-solidus metamorphic conditions (900–1000ºC, ~10 kbar; Cohen et al., 1991), Meen et al. (1992) report depletion on this scale did not occur until the ~3000 Ma event in the WDC.

However, the annealing temperature of zircon is only 600–650ºC (Mezger and Krogstad, 1997), in the upper amphibolite facies at typical crustal thicknesses. Below this temperature, U-rich domains will preferentially accumulate radiation damage to the zircon structure, rendering them open to Pb leakage in later metamorphic events. The zircons in SRG-2 and CH3 all responded differently during the ~3000 Ma event, suggesting a change in tectonic processes around this time which left zircons younger than this age preferentially susceptible to later alteration. The regional scale and nature of this change therefore most likely indicates a metamorphic event with significant variation in crustal depths and P–T conditions, such as initial cratonisation. Pb loss most likely occurred during the next major regional metamorphic episode at ~2550 Ma (e.g., Jayananda et al., 2013b), corresponding to the youngest ages in SRG-2.

If the ~3000 Ma event does mark the start of terrane accumulation and a significant change in tectonic setting in the WDC, clear evidence should be found in the chemical and physical structure of the block. Seismological work by Borah et al. (2014) identified that the lithospheric keel is considerably thicker under the WDC than the EDC, as is the overall thickness of the crust, suggesting cratonisation was of a longer duration in this block, with strong, eclogitic-like material at the base of the crust to provide stability. Hoffmann et al. (2011) considered bulk and trace element distributions in ~3000 Ma TTGs in the WDC which indicate derivation from thickened mafic crust, with mixing between rutile-bearing and rutile-free eclogitic residue. The event which depleted many WDC basement rocks in heat-producing elements at ~3000 Ma left them resistant to both reworking and intrusion by younger granites during later regional metamorphism at ~2550 Ma (Meen et al., 1992). Together, it is clear the ~3000 Ma event marks a critical change in the evolutionary history of the WDC, possibly the onset of ‘plate tectonic’ processes as suggested by large global studies (e.g., Dhuime et al., 2012; Shirey and Richardson, 2011), and its effects have determined the outcome of later intracrustal reworking.

By contrast, the EDC is dominated by 2700–2500 granitoids and greenstone belts which provided the detrital zircons in GLCH-1, with remnants of Meso- to Palaeoarchaean components (Dey et al., 2014b; Jayananda et al., 2000; Maibam et al., 2011). Typical differences between extraction and crystallisation ages in this sample are 400–500 Ma, consistent with the global average (e.g., Lancaster et al., 2011), suggesting ‘modern’ crustal processes were established by this time. For instance, the ~2700 Ma Gadwal greenstone belt preserves whole rock compositions consistent with minimal interaction with mature continental crust, but considerable variation in εHf and εNd values (Khanna et al., 2014). These authors concluded that the Gadwal belt records intra-arc variation, as is observed in modern arcs such as the Aleutians (Yogodzinski et al., 1995; Yogodzinski et al., 2010), rather than mixing. The lack of scatter in εHf in the GLCH-1 zircons therefore reflects derivation from a single, restricted source within one of these belts.

Units of a similar age are also known in the WDC, particularly as felsic volcanic layers (Jayananda et al., 2013a; Kumar et al., 1996; Mohan et al., 2014; Nutman et al., 1996). As such, the abundance of units preserving new and reworked crust in both blocks between 2700–2400 Ma is the result of repeated accretion events concluding with regional metamorphism in both terranes up to the granulite facies at ~2520 Ma during final assembly of the Superia supercontinent (Jayananda et al., 2006, 2013a; Khanna et al., 2014; Peucat et al., 2013). It is this event which remobilised Pb in zircons from all three samples in this study, with the severity of that loss depending on the overall U content of each grain, the nature of any high-U domains within those grains and the metamorphic history each experienced (e.g., Hay and Dempster, 2009b, a; Malusà et al., 2013).

5.3 Correlations with other Archaean cratons

Similarities between Archaean terranes around the globe have led to many suggested correlations and palaeoreconstructions, with the inherent uncertainties increasing as we travel further back into the past. Rogers (1996) suggested the WDC formed the supercontinent Ur, together with the Pilbara and Kaapvaal cratons and East Antarctica, though this view is not entirely accepted (e.g., de Kock et al., 2009). Others have considered potential correlations between sequences in the WDC and the Kaapvaal or Slave cratons (e.g., Bleeker, 2003; Hokada et al., 2013) and the EDC with the Napier complex in East Antarctica and the N Australia craton (e.g., Hollis et al., 2014; Mohanty, 2011). Some authors have also suggested that the N China craton has a magmatic, sedimentological and metamorphic history similar to that of peninsular India, and they were possibly part of the same continent from the Mesoarchaean to the Palaeoproterozoic (Hou et al., 2008; Zhao et al., 2003). Comparing the U–Pb and Hf zircon data from this study with published data from these belts provides another angle on this ongoing debate (Fig. 8a).

The sub-horizontal spread of εHf values around CHUR >3000 Ma is only observed in the three terranes within the Kaapvaal craton (Murchison-Northern Kaapvaal, Barberton North and Barberton South) and the two WDC samples, while the kink in εHf values at ~3000 Ma in SRG-2 is also observed in the three Kaapvaal terranes. Terranes of a similar age elsewhere either appear to record short-duration ('episodic') events with vertical arrays, or form long arrays parallel to $^{176}Lu/^{177}Hf$ evolution lines. While these observations may be an artefact of preservation, it is also possible that the processes controlling crustal growth in the Barberton and Dharwar cratons were different from those elsewhere. The most juvenile εHf values within the sub-horizontal arrays form a line slightly above CHUR that mimics the evolution of the depleted mantle. Over this time frame (~3500–3000 Ma), the difference between extraction age (Hf) and crystallisation age (U–Pb) in these zircons only varies from ~280–320 Ma, suggesting a continuous process of extraction and rapid evolution to zircon-bearing compositions was interrupted only by the onset of cratonisation at ~3000 Ma. In this case, the three main patterns observed in the global zircon data—vertical, horizontal and diagonal—reflect coexisting methods of continental crustal production, and models of early Earth evolution must incorporate them all to be truly representative.

Differences between the Barberton and WDC samples provide more clues to craton formation in the Archaean. Unlike older greenstone belts in the Kaapvaal and Pilbara, the Chitradurga belt (CH3) does not record reworking of pre-existing crust. Juvenile material resembling that in CH3 is only rarely observed in zircons from any other craton, again arguing against a single crustal evolution model (i.e., episodic plumes vs. constant accretion via subduction) in the Palaeo- to Mesoarchaean. However, the Neoarchaean Chitradurga belt is much younger than these other two belts, and the older sample (SRG-2) does provide clear evidence of reworked crust, suggesting accretion via marginal basins was common at this time (e.g., Kröner et al., 2013; Tessalina et al., 2010).

In addition, most Archaean terranes record extensive crustal reworking at ~2700 Ma, thought to record the collisional phase of the Superia supercontinent, followed by relative quiescence (e.g., Campbell and Allen, 2008; Dey, 2013; Nance et al., 2014). While units of this age are abundant in both the Dharwar and Kaapvaal cratons, only the Dharwar craton records significant extraction and metamorphism after ~2700 Ma, reflecting cratonisation of the Kaapvaal at this time (e.g., Poujol et al., 2003; Rajesh et al., 2014). By contrast, the North China craton records significant juvenile extraction at ~2700 Ma, and both crustal reworking and granulite-facies metamorphism due to cratonisation at ~2500 Ma (e.g., Wan et al., 2014; Zhai and Santosh, 2011). These zircons fall on the same extraction lines as GLCH-1 and the southern Indian anorthosites, suggesting extraction of juvenile material was common at this time, but only preserved in those terranes which had yet to cratonise. Therefore, the Dharwar Craton preserves a more complete picture of Archaean crustal processes during this critical period than other terranes, and continental collisions were a prominent feature during the construction of Superia.

Even if two terranes record similar physical processes, they do not necessarily share a consanguineous origin. For instance, the Limpopo belt, immediately to the north of the Barberton terranes, reports more negative zircon εHf values and was derived from a high $^{238}U/^{204}Pb$ (μ) source (Barton, 1996), indicating terranes that are now adjacent need not have been extracted in close proximity to one another and vice versa. In addition, each terrane comprises a different suite of rocks. The Barberton greenstone belt is remarkably undeformed and consists of mafic–ultramafic volcanic rocks, greywackes, shales, cherts, felsic volcaniclastics, sandstones and conglomerates (e.g., Grosch et al., 2011; Kröner et al., 2013; Zeh et al., 2013). By contrast the Sargur belts (SRG-2) are dominated by highly deformed and metamorphosed quartzites, metapelites, metacarbonates, basalts, komatiites and barites (summaries in Jayananda et al., 2008; Meert et al., 2010); conglomerates and greywackes are not reported. These observations suggest that while tectonically linked, they have been geographically separate for most, if not all, of their histories.

6. Conclusions

The Archaean Dharwar craton is a complex terrane comprising many discrete units accreted onto each other through regular collisional events. Significant juvenile crustal extraction events are recorded at ~3.3 and 2.7 Ga, with continuous extraction observed from 3.7–3.3 Ga. Cratonisation in the Dharwar craton occurred in two stages, initiating in the older WDC at ~3000 Ma and the younger EDC at ~2500 Ma, and was completed considerably later than most other Archaean cratons (~2500 Ma vs. ~2700 Ma). Repeated moderate-grade metamorphic events created nanoscale zones of higher U concentrations within the zircon structure, which preferentially leaked Pb during the cratonisation process. Further work is needed to expand the zircon εHf database to permit more complete comparisons between it and more extensive U–Pb and εNd records. Finally, tectonic links are observed between the Barberton terranes of the Kaapvaal craton and the WDC, as well as the North China craton and the EDC, though it does not necessarily require genetic links.

Acknowledgements

PJL thanks J.S. Daly for access to the Neptune at the National Centre for Isotope Geochemistry (NCIG) at University College Dublin, a joint venture of University College Dublin, Trinity College Dublin, University College Cork and National University of Ireland, Galway, funded mainly by Science Foundation Ireland, including Grant No. 04/BR/ES0007/EC07 awarded to J.S. Daly. SD acknowledges Indian School of Mines research grant FRS(13)/2010-11/AGL and Department of Science and Technology (DST), Government of India grant SR/S4/ES-503/2010(G) as well as IGCP-SIDA project 599 (The Changing Early Earth). AM has received a research fellowship through the DST project SR/S4/ES-503/2010(G). Constructive reviews by Bruno Dhuime and an anonymous reviewer greatly improved this paper.

References

Anand, M., Gibson, S.A., Subbarao, K.V., Kelley, S.P., Dickin, A.P., 2003. Early Proterozoic melt generation processes beneath the intra-cratonic Cuddapah Basin, southern India. Journal of Petrology 44, 2139-2171, 10.1093/petrology/egg073.

Balakrishnan, S., Hanson, G.N., Rajamani, V., 1991. Pb and Nd isotope constraints on the origin of high Mg and tholeiitic amphibolites, Kolar Schist Belt, South India. Contributions to Mineralogy and Petrology 107, 279-292, 10.1007/BF00325099.

Barton, J.M., Jr., 1996. The Messina Layered Intrusion, Limpopo Belt, South Africa: An example of *in situ* contamination of an Archean anorthosite complex by continental crust. Precambrian Research 78, 139-150, 10.1016/0301-9268(95)00074-7.

Basu, H., Suryanarayana Sastry, R., Achar, K.K., Umamaheswar, K., Parihar, P.S., 2014. Palaeoproterozoic fluvio-aeolian deposits from the lower Gulcheru Formation, Cuddapah Basin, India. Precambrian Research 246, 321-333, 10.1016/j.precamres.2014.03.011.

Beckinsale, R.D., Drury, S.A., Holt, R.W., 1980. 3,360-Myr old gneisses from the South Indian Craton. Nature 283, 469-470, 10.1038/283469a0.

Bhaskar Rao, Y.J., Griffin, W.L., Ketchum, J.W.F., Pearson, N.J., Beyer, E., O'Reilly, S.Y., 2008. An outline of juvenile crust formation and recycling history in the Archaean Western Dharwar craton, from zircon *in situ* U–Pb dating and Hf-isotopic compositions. Geochimica et Cosmochimica Acta 72, A81.

Bhaskar Rao, Y.J., Janardhan, A.S., Kumar, T.V., Narayana, B.L., Dayal, A.M., Taylor, P.N., Chetty, T.R.K., 2003. Sm–Nd model ages and Rb–Sr isotopic systematics of charnockites and gneisses across the Cauvery shear zone, Southern India: Implications for the Archaean-Neoproterozoic terrane boundary in the Southern Granulite Terrain, In: Ramakrishnan, M. (Ed.), Tectonics of Southern Granulite Terrain: Kuppam-Palani Geotransect. Geological Society of India, Memoirs, 50, pp. 297-317.

Bhaskar Rao, Y.J., Pantulu, G.V.C., Reddy, V.D., Gopalan, K., 1995. Time of early sedimentation and volcanism in the Proterozoic Cuddapah basin, South India: Evidence from the Rb–Sr age of Pulivendla mafic sill, In: Devaraju, T.C. (Ed.), Dyke swarms of peninsular India. Memoir of the Geological Society of India, 33, pp. 329-338.

Bickford, M.E., Saha, D., Schieber, J., Kamenov, G., Russell, A., Basu, A., 2013. New U–Pb ages of zircons in the Owk Shale (Kurnool Group) with reflections on Proterozoic porcellanites in India. Journal of the Geological Society of India 82, 207-216.

Bleeker, W., 2003. The late Archean record: A puzzle in ca. 35 pieces. Lithos 71, 99-134, 10.1016/j.lithos.2003.07.003.

Borah, K., Rai, S.S., Gupta, S., Prakasam, K.S., Kumar, S., Sivaram, K., 2014. Preserved and modified mid-Archean crustal blocks in Dharwar craton: Seismological evidence. Precambrian Research 246, 16-34, 10.1016/j.precamres.2014.02.003.

Bouvier, A., Vervoort, J.D., Patchett, P.J., 2008. The Lu–Hf and Sm–Nd isotopic composition of CHUR: Constraints from unequilibrated chondrites and implications for the bulk composition of terrestrial planets. Earth and Planetary Science Letters 273, 48-57, 10.1016/j.epsl.2008.06.010.

Brandt, S., Raith, M.M., Schenk, V., Sengupta, P., Srikantappa, C., Gerdes, A., 2014. Crustal evolution of the Southern Granulite Terrane, south India: New geochronological and geochemical data for felsic orthogneisses and granites. Precambrian Research 246, 91-122, 10.1016/j.precamres.2014.01.007.

Campbell, I.H., Allen, C.M., 2008. Formation of supercontinents linked to increases in atmospheric oxygen. Nature Geoscience 1, 554-558, 10.1038/ngeo259.

Chadwick, B., Vasudev, V.N., Hegde, G.V., 2000. The Dharwar craton, southern India, interpreted as the result of Late Archaean oblique convergence. Precambrian Research 99, 91-111, 10.1016/S0301-9268(99)00055-8.

Chadwick, B., Vasudev, V.N., Hegde, G.V., Nutman, A.P., 2007. Structure and SHRIMP U–Pb zircon ages of granites adjacent to the Chitradurga Schist belt: Implications for neoarchaean convergence in the Dharwar Craton, Southern India. Journal of the Geological Society of India 69, 5-24.
Chardon, D., Jayananda, M., Peucat, J.-J., 2011. Lateral constrictional flow of hot orogenic crust: Insights from the Neoarchean of south India, geological and geophysical implications for orogenic plateaux. Geochemistry, Geophysics, Geosystems 12, Q02005, 10.1029/2010GC003398.
Chardon, D., Peucat, J.-J., Jayananda, M., Choukroune, P., Fanning, C.M., 2002. Archean granite-greenstone tectonics at Kolar (South India): Interplay of diapirism and bulk inhomogeneous contraction during juvenile magmatic accretion. Tectonics 21, 1016, 10.1029/2001TC901032.
Chauvel, C., Garçon, M., Bureau, S., Besnault, A., Jahn, B.-m., Ding, Z., 2014. Constraints from loess on the Hf-Nd isotopic composition of the upper continental crust. Earth and Planetary Science Letters 388, 48-58, 10.1016/j.epsl.2013.11.045.
Cohen, A.S., O'Nions, R.K., O'Hara, M.J., 1991. Chronology and mechanism of depletion in Lewisian granulites. Contributions to Mineralogy and Petrology 106, 142-153, 10.1007/BF00306430.
de Kock, M.O., Evans, D.A.D., Beukes, N.J., 2009. Validating the existence of Vaalbara in the Neoarchean. Precambrian Research 174, 145-154, 10.1016/j.precamres.2009.07.002.
Devaraju, T.C., Huhma, H., Sudhakara, T.L., Kaukonen, R.J., Alapieti, T.T., 2007. Petrology, geochemistry, model Sm–Nd ages and petrogenesis of the granitoids of the northern block of Western Dharwar Craton. Journal of the Geological Society of India 70, 889-911.
Dey, S., 2013. Evolution of Archaean crust in the Dharwar craton: The Nd isotope record. Precambrian Research 227, 227-246, 10.1016/j.precamres.2009.07.002.
Dey, S., Gajapathi Rao, R., Gorikhan, R.A., Veerabhaskar, D., Kumar, S., Kumar, M.K., 2003. Geochemistry and origin of Northern Closepet Granite from Gudur-Guledagudda area, Bagalkot District, Karnataka. Journal of the Geological Society of India 62, 152-168.
Dey, S., Nandy, J., Choudhary, A.K., Liu, Y., Zong, K., 2014a. Neoarchaean crustal growth by combined arc–plume action: Evidence from the Kadiri Greenstone Belt, eastern Dharwar craton, India, In: Roberts, N.M.W., van Kranendonk, M.J., Parman, S.W., Shirey, S.B., Clift, P.D. (Eds.), Continent formation through time. Geological Society of London Special Publications, 389, 10.1144/SP389.3.
Dey, S., Nandy, J., Choudhary, A.K., Liu, Y., Zong, K., 2014b. Origin and evolution of granitoids associated with the Kadiri greenstone belt, eastern Dharwar craton: A history of orogenic to anorogenic magmatism. Precambrian Research 246, 64-90, 10.1016/j.precamres.2014.02.007.
Dey, S., Pandey, U.K., Rai, A.K., Chaki, A., 2012. Geochemical and Nd isotope constraints on petrogenesis of granitoids from NW part of the eastern Dharwar craton: Possible implications for late Archaean crustal accretion. Journal of Asian Earth Sciences 45, 40-56, 10.1016/j.jseaes.2011.09.013.
Dey, S., Rai, A.K., Chaki, A., 2009. Geochemistry of granitoids of Bilgi area, northern part of eastern Dharwar craton, southern India: Example of transitional TTGs derived from depleted source. Journal of the Geological Society of India 73, 854-870.
Dhuime, B., Hawkesworth, C.J., Cawood, P.A., 2011. When continents formed. Science 331, 154-155, 10.1126/science.1201245.
Dhuime, B., Hawkesworth, C.J., Cawood, P.A., Storey, C.D., 2012. A change in the geodynamics of continental growth 3 billion years ago. Science 335, 1334-1336, 10.1126/science.1216066.

Fedo, C.M., Sircombe, K.N., Rainbird, R.H., 2003. Detrital zircon analysis of the sedimentary record, In: Hanchar, J.M., Hoskin, P.W.O. (Eds.), Zircon. Reviews in mineralogy and geochemistry, pp. 277-304.
French, J.E., Heaman, L.M., 2010. Precise U–Pb dating of Paleoproterozoic mafic dyke swarms of the Dharwar craton, India: Implications for the existence of the Neoarchean supercraton Sclavia. Precambrian Research 183, 416-441, 10.1016/j.precamres.2010.05.003.
French, J.E., Heaman, L.M., Chacko, T., Srivastava, R.K., 2008. 1891–1883 Ma Southern Bastar–Cuddapah mafic igneous events, India: A newly recognized large igneous province. Precambrian Research 160, 308-322, 10.1016/j.precamres.2007.08.005.
Geological Survey of India, 2006. Southern part of the peninsula, In: Guha, D., Pyne, T.K., Mallick, S., Basu Chakrabarti, C. (Eds.), Precambrian, 4th ed. A manual of the geology of India, 1.
Griffin, W.L., Wang, X., Jackson, S.E., Pearson, N.J., O'Reilly, S.Y., Xu, X., Zhou, X., 2002. Zircon chemistry and magma mixing, SE China: *In situ* analysis of Hf isotopes, Tonglu and Pingtan igneous complexes. Lithos 61, 237-269, 10.1016/j.lithos.2003.07.003.
Grosch, E.G., Košler, J., McLoughlin, N., Drost, K., Sláma, J., Pedersen, R.B., 2011. Paleoarchean detrital zircon ages from the earliest tectonic basin in the Barberton Greenstone Belt, Kaapvaal craton, South Africa. Precambrian Research 191, 85-99, 10.1016/j.precamres.2011.09.003.
Gupta, S., Rai, S.S., Prakasam, K.S., Srinagesh, D., Bansal, B.K., Chadha, R.K., Priestley, K., Gaur, V.K., 2003. The nature of the crust in southern India: Implications for Precambrian crustal evolution. Geophysical Research Letters 30, 1419, 10.1029/2002GL016770.
Halpin, J.A., Daczko, N.R., Milan, L.A., Clarke, G.L., 2012. Decoding near-concordant U–Pb zircon ages spanning several hundred million years: Recrystallisation, metamictisation or diffusion? Contributions to Mineralogy and Petrology 163, 67-85, 10.1007/s00410-011-0659-7.
Hawkesworth, C.J., Cawood, P.A., Kemp, A.I.S., Storey, C.D., Dhuime, B., 2009. A matter of preservation. Science 323, 49-50, 10.1126/science.1168549.
Hawkesworth, C.J., Dhuime, B., Pietranik, A.B., Cawood, P.A., Kemp, A.I.S., Storey, C.D., 2010. The generation and evolution of the continental crust. Journal of the Geological Society 167, 229-248, 10.1144/0016-76492009-072
Hawkesworth, C.J., Kemp, A.I.S., 2006. Using hafnium and oxygen isotopes in zircons to unravel the record of crustal evolution. Chemical Geology 226, 144-162, 10.1016/j.chemgeo.2005.09.018.
Hay, D.C., Dempster, T.J., 2009a. Zircon alteration, formation and preservation in sandstones. Sedimentology 56, 2175-2191, 10.1111/j.1365-3091.2009.01075.x.
Hay, D.C., Dempster, T.J., 2009b. Zircon behaviour during low-temperature metamorphism. Journal of Petrology 50, 571-589, 10.1093/petrology/egp011.
Hoffmann, J.E., Münker, C., Næraa, T., Rosing, M.T., Herwartz, D., Garbe-Schönberg, D., Svahnberg, H., 2011. Mechanisms of Archean crust formation inferred from high-precision HFSE systematics in TTGs. Geochimica et Cosmochimica Acta 75, 4157-4178, 10.1016/j.gca.2011.04.027.
Hokada, T., Horie, K., Satish-Kumar, M., Ueno, Y., Nasheeth, A., Mishima, K., Shiraishi, K., 2013. An appraisal of Archaean supracrustal sequences in Chitradurga Schist Belt, western Dharwar craton, southern India. Precambrian Research 227, 99-119, 10.1016/j.precamres.2012.04.006.
Hollis, J.A., Carson, C.J., Glass, L.M., Kositcin, N., Scherstén, A., Worden, K.E., Armstrong, R.A., Yaxley, G.M., Kemp, A.I.S., 2014. Detrital zircon U–Pb-Hf and O isotope character of the Cahill Formation and Nourlangie Schist, Pine Creek Orogen: Implications for the tectonic

correlation and evolution of the North Australian Craton. Precambrian Research 246, 35-53, 10.1016/j.precamres.2009.08.010.
Hou, G., Santosh, M., Qian, X., Lister, G.S., Li, J., 2008. Configuration of the Late Paleoproterozoic supercontinent Columbia: Insights from radiating mafic dyke swarms. Gondwana Research 14, 395-409, 10.1016/j.gr.2012.07.008.
Jackson, S.E., Pearson, N.J., Griffin, W.L., Belousova, E.A., 2004. The application of laser ablation-inductively coupled plasma-mass spectrometry to in situ U-Pb zircon geochronology. Chemical Geology 211, 47-69, 10.1016/j.chemgeo.2004.06.017.
Janardhan, A.S., 1994. Ancient supracrustals of sargur type: A review, Geo Karnataka. Mysore Geological Department Centenary Volume, pp. 36-44.
Janardhan, A.S., Newton, R.C., Hansen, E.C., 1982. The transformation of amphibolite facies gneiss to charnockite in southern Karnataka and northern Tamil Nadu, India. Contributions to Mineralogy and Petrology 79, 130-149, 10.1007/BF01132883.
Jayananda, M., Banerjee, M., Pant, N.C., Dasgupta, S., Kano, T., Mahesha, N., Mahabaleswar, B., 2012. 2.62 Ga high-temperature metamorphism in the central part of the Eastern Dharwar Craton: Implications for late Archaean tectonothermal history. Geological Journal 47, 213-236, 10.1002/gj.1308.
Jayananda, M., Chardon, D., Peucat, J.-J., Capdevila, R., 2006. 2.61 Ga potassic granites and crustal reworking in the western Dharwar craton, southern India: Tectonic, geochronologic and geochemical constraints. Precambrian Research 150, 1-26, 10.1016/j.precamres.2006.05.004.
Jayananda, M., Kano, T., Peucat, J.-J., Channabasappa, S., 2008. 3.35 Ga komatiite volcanism in the western Dharwar craton, southern India: Constraints from Nd isotopes and whole-rock geochemistry. Precambrian Research 162, 160-179, 10.1016/j.precamres.2007.07.010.
Jayananda, M., Martin, H., Peucat, J.-J., Mahabaleswar, B., 1995. Late Archaean crust-mantle interactions: Geochemistry of LREE-enriched mantle derived magmas. Example of the Closepet batholith, southern India. Contributions to Mineralogy and Petrology 119, 314-329, 10.1007/BF00307290.
Jayananda, M., Moyen, J.-F., Martin, H., Peucat, J.-J., Auvray, B., Mahabaleswar, B., 2000. Late Archaean (2550–2520 Ma) juvenile magmatism in the Eastern Dharwar craton, southern India: Constraints from geochronology, Nd-Sr isotopes and whole rock geochemistry. Precambrian Research 99, 225-254, 10.1016/S0301-9268(99)00063-7.
Jayananda, M., Peucat, J.-J., Chardon, D., Rao, B.K., Fanning, C.M., Corfu, F., 2013a. Neoarchean greenstone volcanism and continental growth, Dharwar craton, southern India: Constraints from SIMS U–Pb zircon geochronology and Nd isotopes. Precambrian Research 227, 55-76, 10.1016/j.precamres.2012.05.002.
Jayananda, M., Tsutsumi, Y., Miyazaki, T., Gireesh, R.V., Kapfo, K.-u., Tushipokla, Hidaka, H., Kano, T., 2013b. Geochronological constraints on Meso- and Neoarchean regional metamorphism and magmatism in the Dharwar craton, southern India. Journal of Asian Earth Sciences 78, 18-38, 10.1016/j.jseaes.2013.04.033.
Jeffries, T.E., Fernandez-Suarez, J., Corfu, F., Alonso, G.G., 2003. Advances in U–Pb geochronology using a frequency quintupled Nd:YAG based laser ablation system (λ = 213 nm) and quadrupole based ICP-MS. Journal of Analytical Atomic Spectrometry 18, 847-855, 10.1039/B300929G.
Kaur, P., Zeh, A., Chaudhri, N., Gerdes, A., Okrusch, M., 2011. Archaean to Palaeoproterozoic crustal evolution of the Aravalli mountain range, NW India, and its hinterland: The U–Pb and Hf isotope record of detrital zircon. Precambrian Research 187, 155-164, 10.1016/j.precamres.2011.03.005.

Kaur, P., Zeh, A., Chaudhri, N., Gerdes, A., Okrusch, M., 2013. Nature of magmatism and sedimentation at a Columbia active margin: Insights from combined U−Pb and Lu−Hf isotope data of detrital zircons from NW India. Gondwana Research 23, 1040-1052, 10.1016/j.gr.2012.07.008.

Khanna, T.C., Bizimis, M., Yogodzinski, G.M., Mallick, S., 2014. Hafnium–neodymium isotope systematics of the 2.7 Ga Gadwal greenstone terrane, Eastern Dharwar craton, India: Implications for the evolution of the Archean depleted mantle. Geochimica et Cosmochimica Acta 127, 10-24, 10.1016/j.gca.2013.11.024.

Kooijman, E., Upadhyay, D., Mezger, K., Raith, M.M., Berndt, J., Srikantappa, C., 2011. Response of the U–Pb chronometer and trace elements in zircon to ultrahigh-temperature metamorphism: The Kadavur anorthosite complex, southern India. Chemical Geology 290, 177-188, 10.1016/j.chemgeo.2011.09.013.

Košler, J., Forst, L., Sláma, J., 2008. LamDate and LamTool: Spreadsheet-based data reduction for laser ablation ICP-MS, In: Sylvester, P.J. (Ed.), Laser ablation in the Earth Sciences: Current practices and outstanding issues. Short Course Series, 40, pp. 315-317.

Kröner, A., Hoffmann, J.E., Xie, H., Wu, F., Münker, C., Hegner, E., Wong, J., Wan, Y., Liu, D., 2013. Generation of early Archaean felsic greenstone volcanic rocks through crustal melting in the Kaapvaal, craton, southern Africa. Earth and Planetary Science Letters 381, 188-197, 10.1016/j.epsl.2013.08.029.

Kumar, A., Bhaskar Rao, Y.J., Sivaraman, T.V., Gopalan, K., 1996. Sm–Nd ages of Archaean metavolcanics of the Dharwar craton, South India. Precambrian Research 80, 205-216, 10.1016/S0301-9268(96)00015-0.

Kumar, A., Hamilton, M.A., Halls, H.C., 2012. A Paleoproterozoic giant radiating dyke swarm in the Dharwar Craton, southern India. Geochemistry Geophysics Geosystems 13, Q0100X, 10.1029/2011GC003926.

Lancaster, P.J., Storey, C.D., Hawkesworth, C.J., Dhuime, B., 2011. Understanding the roles of crustal growth and preservation in the detrital zircon record. Earth and Planetary Science Letters 305, 405-412, 10.1016/j.epsl.2011.03.022.

Ludwig, K.R., 2003. User's Manual for Isoplot 3.00, A Geochronological Toolkit for Microsoft Excel. Berkeley Geochronology Special Publication 4, Berkeley, CA.

Maibam, B., Goswami, J.N., Srinivasan, R., 2011. Pb–Pb zircon ages of Archaean metasediments and gneisses from the Dharwar craton, southern India: Implications for the antiquity of the eastern Dharwar craton. Journal of Earth System Science 120, 643-661, 10.1007/s12040-011-0094-1.

Malusà, M.G., Carter, A., Limoncelli, M., Villa, I.M., Garzanti, E., 2013. Bias in detrital zircon geochronology and thermochronometry. Chemical Geology 359, 90-107, 10.1016/j.chemgeo.2011.09.013.

Mange, M.A., Maurer, H.F.W., 1992. Heavy minerals in colour. Chapman and Hall, London.

Manikyamba, C., Kerrich, R., 2012. Eastern Dharwar Craton, India: Continental lithosphere growth by accretion of diverse plume and arc terranes. Geoscience Frontiers 3, 225-240, 10.1016/j.gsf.2011.11.009.

Meen, J.K., Rogers, J.J.W., Fullagar, P.D., 1992. Lead isotopic compositions of the Western Dharwar craton, southern India: Evidence for distinct Middle Archean terranes in a Late Archean craton. Geochimica et Cosmochimica Acta 56, 2455-2470, 10.1016/0016-7037(92)90202-T.

Meert, J.G., Pandit, M.K., Pradhan, V.R., Banks, J., Sirianni, R., Stroud, M., Newstead, B., Gifford, J., 2010. Precambrian crustal evolution of peninsular India: A 3.0 billion year odyssey. Journal of Asian Earth Sciences 39, 483-515, 10.1016/j.gsf.2011.11.009.

Mezger, K., Krogstad, E.J., 1997. Interpretation of discordant U–Pb zircon ages: An evaluation. Journal of Metamorphic Geology 15, 127-140, 10.1111/j.1525-1314.1997.00008.x.

Mohan, M.R., Piercey, S.J., Kamber, B.S., Sarma, D.S., 2013a. Subduction related tectonic evolution of the Neoarchean eastern Dharwar Craton, southern India: New geochemical and isotopic constraints. Precambrian Research 227, 204-226, 10.1016/j.precamres.2012.06.012.

Mohan, M.R., Sarma, D.S., McNaughton, N.J., Fletcher, I.R., Wilde, S.A., Siddiqui, M.A., Rasmussen, B., Krapez, B., Gregory, C.J., Kamo, S.L., 2014. SHRIMP zircon and titanite U–Pb ages, Lu–Hf isotope signatures and geochemical constraints for ~2.56 Ga granitic magmatism in western Dharwar Craton, southern India: Evidence for short-lived Neoarchean episodic crustal growth. Precambrian Research 243, 197-220, 10.1016/j.precamres.2013.12.017.

Mohan, M.R., Satyanarayanan, M., Santosh, M., Sylvester, P.J., Tubrett, M.N., Lam, R., 2013b. Neoarchean suprasubduction zone arc magmatism in southern India: Geochemistry, zircon U–Pb geochronology and Hf isotopes of the Sittampundi Anorthosite Complex. Gondwana Research 23, 539-557, 10.1016/j.gr.2012.04.004.

Mohanty, S., 2011. Palaeoproterozoic assembly of the Napier Complex, Southern India and Western Australia: Implications for the evolution of the Cuddapah basin. Gondwana Research 20, 344-361, 10.1016/j.gr.2011.03.009.

Mojzsis, S.J., Cates, N.L., Caro, G., Trail, D., Abramov, O., Guitreau, M., Blichert-Toft, J., Hopkins, M.D., Bleeker, W., 2014. Component geochronology in the polyphase ca. 3920 Ma Acasta Gneiss. Geochimica et Cosmochimica Acta 133, 68-96, 10.1016/j.gca.2014.02.019.

Moyen, J.-F., Martin, H., Jayananda, M., 2001. Multi-element geochemical modelling of crust–mantle interactions during late-Archaean crustal growth: The Closepet granite (South India). Precambrian Research 112, 87-105, 10.1016/S0301-9268(01)00171-1.

Moyen, J.-F., Martin, H., Jayananda, M., Auvray, B., 2003. Late Archaean granites: A typology based on the Dharwar Craton (India). Precambrian Research 127, 103-123, 10.1016/S0301-9268(03)00183-9.

Mukherjee, R., Mondal, S.K., Frei, R., Rosing, M.T., Waight, T.E., Zhong, H., Kumar, G.R.R., 2012. The 3.1 Ga Nuggihalli chromite deposits, Western Dharwar craton (India): Geochemical and isotopic constraints on mantle sources, crustal evolution and implications for supercontinent formation and ore mineralization. Lithos 155, 392-409, http://dx.doi.org/10.1016/j.lithos.2012.10.001.

Næraa, T., Scherstén, A., Rosing, M.T., Kemp, A.I.S., Hoffmann, J.E., Kokfelt, T.F., Whitehouse, M.J., 2012. Hafnium isotope evidence for a transition in the dynamics of continental growth 3.2Gyr ago. Nature 485, 627-630, doi:10.1038/nature11140.

Nance, R.D., Murphy, J.B., Santosh, M., 2014. The supercontinent cycle: A retrospective essay. Gondwana Research 25, 4-29, 10.1016/j.gr.2012.12.026.

Naqvi, S.M., Khan, R.M.K., Manikyamba, C., Mohan, M.R., Khanna, T.C., 2006. Geochemistry of the Neoarchaean high-Mg basalts, boninites and adakites from the Kushtagi–Hungund greenstone belt of the Eastern Dharwar Craton (EDC): Implications for the tectonic setting. Journal of Asian Earth Sciences 27, 25-44, 10.1016/j.jseaes.2005.01.006.

Nutman, A.P., Chadwick, B., Ramakrishnan, M., Viswanathan, M.N., 1992. SHRIMP U–Pb ages of detrital zircon in Sargur supracrustal rocks in western Karnataka, southern India. Journal of the Geological Society of India 39, 367-374.

Nutman, A.P., Chadwick, B., Rao, B.K., Vasudev, V.N., 1996. SHRIMP U–Pb zircon ages of acid volcanic rocks in the Chitradurga and Sandur groups, and granites adjacent to the Sahdur schist belt, Karnataka. Journal of the Geological Society of India 47, 153-164.

Peucat, J.-J., Jayananda, M., Chardon, D., Capdevila, R., Fanning, C.M., Paquette, J.-L., 2013. The lower crust of the Dharwar Craton, Southern India: Patchwork of Archean granulitic domains. Precambrian Research 227, 4-28, 10.1016/j.precamres.2012.06.009.
Peucat, J.-J., Mahabaleswar, B., Jayananda, M., 1993. Age of younger tonalitic magmatism and granulitic metamorphism in the South Indian transition zone (Krishnagiri area): Comparison with older Peninsular gneisses from the Gorur–Hassan area. Journal of Metamorphic Geology 11, 879-888, 10.1111/j.1525-1314.1993.tb00197.x.
Poujol, M., Robb, L.J., Anhaeusser, C.R., Gericke, B., 2003. A review of the geochronological constraints on the evolution of the Kaapvaal Craton, South Africa. Precambrian Research 127, 181-213, 10.1016/S0301-9268(03)00187-6.
Praveen, M.N., Santosh, M., Yang, Q.Y., Zhang, Z.C., Huang, H., Singanenjam, S., Sajinkumar, K.S., 2014. Zircon U–Pb geochronology and Hf isotope of felsic volcanics from Attappadi, southern India: Implications for Neoarchean convergent margin tectonics. Gondwana Research 26, 907-924, 10.1016/j.gr.2013.08.004.
Raith, M., Raase, P., Ackermand, D., Lal, R.K., 1983. Regional geothermobarometry in the granulite facies terrane of South India. Transactions of the Royal Society of Edinburgh: Earth Sciences 73, 221-244, 10.1017/S026359330000969X.
Rajesh, H.M., Santosh, M., Wan, Y., Liu, D., Liu, S.J., Belyanin, G.A., 2014. Ultrahigh temperature granulites and magnesian charnockites: Evidence for Neoarchean accretion along the northern margin of the Kaapvaal Craton. Precambrian Research 246, 150-159, 10.1016/j.precamres.2014.03.001.
Rogers, J.J.W., 1996. A history of continents in the past three billion years. Journal of Geology 104, 91-107.
Saha, D., Mazumder, R., 2012. An overview of the Palaeoproterozoic geology of Peninsular India, and key stratigraphic and tectonic issues, In: Mazumder, R., Saha, D. (Eds.), Palaeoproterozoic of India. Geological Society, London, Special Publications, 365, pp. 5-29, 10.1144/SP365.2.
Saha, D., Tripathy, V., 2012. Palaeoproterozoic sedimentation in the Cuddapah Basin, south India and regional tectonics: A review, In: Mazumder, R., Saha, D. (Eds.), Palaeoproterozoic of India. Geological Society, London, Special Publication, 365, pp. 161-184.
Santosh, M., Yang, Q.-Y., Shaji, E., Tsunogae, T., Mohan, M.R., Satyanarayanan, M., 2014. An exotic Mesoarchean microcontinent: The Coorg Block, southern India. Gondwana Research In press, 10.1016/j.gr.2013.10.005.
Sarma, D.S., McNaughton, N.J., Belousova, E.A., Ram Mohan, M., Fletcher, I.R., 2012. Detrital zircon U–Pb ages and Hf-isotope systematics from the Gadag Greenstone Belt: Archean crustal growth in the western Dharwar Craton, India. Gondwana Research 22, 843-854, 10.1016/j.gr.2012.04.001.
Shirey, S.B., Kamber, B.S., Whitehouse, M.J., Mueller, P.A., Basu, A.R., 2008. A review of the isotopic and trace element evidence for mantle and crustal processes in the Hadean and Archean: Implications for the onset of plate tectonic subduction, In: Condie, K.C., Pease, V. (Eds.), When did plate tectonics begin on planet Earth? Geological Society of America Special Papers, 440, pp. 1-29.
Shirey, S.B., Richardson, S.H., 2011. Start of the Wilson cycle at 3 Ga shown by diamonds from subcontinental mantle. Science 333, 434-436, 10.1126/science.1206275.
Sláma, J., Košler, J., Condon, D.J., Crowley, J.L., Gerdes, A., Hanchar, J.M., Horstwood, M.S.A., Morris, G.A., Nasdala, L., Norberg, N., Schaltegger, U., Schoene, B., Tubrett, M.N., Whitehouse, M.J., 2008. Plešovice zircon — A new natural reference material for U–Pb and Hf isotopic microanalysis. Chemical Geology 249, 1-35, 10.1016/j.chemgeo.2007.11.005.

Söderlund, U., Patchett, P.J., Vervoort, J.D., Isachsen, C.E., 2004. The ^{176}Lu decay constant determined by Lu–Hf and U–Pb isotope systematics of Precambrian mafic intrusions. Earth and Planetary Science Letters 219, 311-324, 10.1016/S0012-821X(04)00012-3.
Srinivasan, R., Ojakangas, R.W., 1986. Sedimentology of quartz-pebble conglomerates and quartzites of the Archean Bababudan Group, Dharwar Craton, South India: Evidence for early crustal stability. The Journal of Geology 94, 199-214.
Suresh, G., Ananthanarayana, R., Hanumanthu, R.C., Ghosh, S., Anil Kumar, A., Reddy, K.V.S., 2010. Geology of Pulikonda and Dancherla alkaline complexes, Andhra Pradesh. Journal of the Geological Society of India 75, 576-595.
Swaminath, J., Ramakrishnan, M., 1981. Early Precambrian supracrustals of southern Karnataka. Geological Survey of India, Memoirs, 112.
Tessalina, S.G., Bourdon, B., Van Kranendonk, M., Birck, J.-L., Philippot, P., 2010. Influence of Hadean crust evident in basalts and cherts from the Pilbara Craton. Nature Geoscience 3, 214-217, 10.1038/ngeo772.
Vermeesch, P., 2012. On the visualisation of detrital age distributions. Chemical Geology 312-313, 190-194, 10.1016/j.chemgeo.2012.04.021.
Wan, Y., Xie, S., Yang, C., Kröner, A., Ma, M., Dong, C., Du, L., Xie, H., Liu, D., 2014. Early Neoarchean (~2.7 Ga) tectono-thermal events in the North China Craton: A synthesis. Precambrian Research 247, 45-63, 10.1016/j.precamres.2014.03.019.
Whitehouse, M.J., Kemp, A.I.S., 2010. On the difficulty of assigning crustal residence, magmatic protolith and metamorphic ages to Lewisian granulites: Constraints from combined *in situ* U–Pb and Lu–Hf isotopes, In: Law, R.D., Butler, R.W.H., Holdsworth, R.E., Krabbendam, M., Strachan, R.A. (Eds.), Continental tectonics and mountain building: The legacy of Peach and Horne. Geological Society, London, Special Publications, 335, pp. 81-101, 10.1144/SP335.5.
Wiedenbeck, M., Hanchar, J.M., Peck, W.H., Sylvester, P.J., Valley, J.W., Whitehouse, M.J., Kronz, A., Morishita, Y., Nasdala, L., Fiebig, J., Franchi, I., Girard, J.P., Greenwood, R.C., Hinton, R.W., Kita, N.T., Mason, P.R.D., Norman, M., Ogasawara, M., Piccoli, P.M., Rhede, D., Satoh, H., Schulz-Dobrick, B., Skår, Ø., Spicuzza, M.J., Terada, K., Tindle, A., Togashi, S., Vennemann, T., Xie, Q., Zheng, Y.-F., 2004. Further characterisation of the 91500 zircon crystal. Geostandards and Geoanalytical Research 28, 9-39, 10.1111/j.1751-908X.2004.tb01041.x.
Woodhead, J., Hergt, J., Shelley, M., Eggins, S., Kemp, R., 2004. Zircon Hf-isotope analysis with an excimer laser, depth profiling, ablation of complex geometries, and concomitant age estimation. Chemical Geology 209, 121-135, 10.1016/j.chemgeo.2004.04.026.
Yogodzinski, G.M., Kay, R.W., Volynets, O.N., Koloskov, A.V., Kay, S.M., 1995. Magnesian andesite in the western Aleutian Komandorsky region: Implications for slab melting and processes in the mantle wedge. Geological Society of America Bulletin 107, 505-519, 10.1130/0016-7606(1995)107<0505:MAITWA>2.3.CO;2.
Yogodzinski, G.M., Vervoort, J.D., Brown, S.T., Gerseny, M., 2010. Subduction controls of Hf and Nd isotopes in lavas of the Aleutian island arc. Earth and Planetary Science Letters 300, 226-238, 10.1016/j.epsl.2010.09.035.
Zeh, A., Gerdes, A., Heubeck, C., 2013. U–Pb and Hf isotope data of detrital zircons from the Barberton Greenstone Belt: Constraints on provenance and Archaean crustal evolution. Journal of the Geological Society 170, 215-223, 10.1144/jgs2011-162.
Zhai, M.-G., Santosh, M., 2011. The early Precambrian odyssey of the North China Craton: A synoptic overview. Gondwana Research 20, 6-25, 10.1016/j.epsl.2010.09.035.
Zhao, G., Sun, M., Wilde, S.A., 2003. Correlations between the Eastern Block of the North China Craton and the South Indian Block of the Indian Shield: An Archaean to

Palaeoproterozoic link. Precambrian Research 122, 201-233, 10.1016/S0301-9268(02)00212-7.

Figure captions:

Figure 1: Geological map of the Dharwar craton (modified after the Vasundhara Project, Geological Survey of India, 1994) showing the location of samples. CSZ - Chitradurga shear zone, CGL - Closepet Granite. Sargur-type schist belts: B - Banasandra, G - Ghattihosahalli, Hn - Holenarasipur, J - J.C. Pura, K - Kalyadi, N - Nuggihalli, Sg - Sargur. Dharwar-type schist belts: Bb - Bababudan, C - Chitradurga, Ga - Gadag, Ku - Kudremukh, S - Sandur, Sh - Shimoga. Kolar-type schist belts: Gd - Gadwal, H - Hutti, Ka - Kadiri, HK - Hungund-Kushtagi, Ko - Kolar, R - Ramagiri, Rc - Raichur, V - Veligallu.

Figure 2. Photomicrographs of samples, all in XN. (a) SRG-2 from the Sargur belt. Deformed quartzite showing parallel alignment of muscovite layers imparting a distinct foliation. (b) CH3 from the Bababudan Group, Chitradurga belt. Deformed quartzite consisting dominantly of quartz with subordinate thin muscovite flakes, the latter arranged in thin subparallel layers defining a foliation. (c) GLCH-1 from the Gulcheru Formation, Cuddapah basin. A quartz arenite consisting of very coarse sand to granule-sized rounded to subrounded grains of quartz (both poly- and mono-crystalline) and chert (at the centre). Interstitial places are filled with fine sands of quartz.

Figure 3: Typical CL images from zircons in this study, indicating analytical locations and resulting data. Solid ellipses - U–Pb. Dashed circles - Hf. Data indicated as grain name (G), $^{207}Pb/^{206}Pb$ age ±2σ, and εHf ±2σ, calculated at the indicated U–Pb age; % disc. indicates discordance when >10%.

Figure 4: Concordia diagrammes for zircons from the three samples in this study, plotted at 2σ. Histogram and kernel density estimate curve of ages <10% in (a) plotted using the DensityPlotter tool of Vermeesch (2012). Core - innermost growth zone. Mantle - intermediate growth zone(s). Rim - outermost growth zone. Whole - no obvious internal zoning.

Figure 5: Plots of $^{207}Pb/^{206}Pb$ ages vs. U, Pb and Th concentrations in zircons from this study. Top row - U. Middle row - Pb. Bottom row - Th.

Figure 6: Plot of $^{176}Hf/^{177}Hf$ vs. U–Pb age for all data in this study, coded for growth zones as in Fig. 4, except mantles and rims are grouped as overgrowths (overs). Uncertainties plotted at 2σ.

Figure 7: Plot of εHf vs. U–Pb age for all data with U–Pb ages <10% discordant from this study, coded for growth zone as in Fig. 6. Uncertainties plotted at 2σ. Top: εHf values calculated using the measured $^{207}Pb/^{206}Pb$ ages. Bottom: εHf values calculated at the best estimate of the crystallisation age, based on the evidence for Pb loss in Figs. 4 and 6 (see text for discussion). CHUR - chondritic reservoir (bulk Earth). DM - depleted mantle; Griffin et al. (2002). NC - new crust; Dhuime et al. (2011). S08 - mantle model of Shirey et al. (2008).

Figure 8: Plot of εHf vs. U–Pb age for data <10% discordant in this study, plotted against published data from other Archaean terranes (references in the Supplementary Material). Data from this study are plotted at the best estimate U–Pb crystallisation ages, as discussed in

the text. Dark dashed lines indicate evolution of parental rocks with a $^{176}Lu/^{177}Hf$ of 0.015 extracted from the depleted mantle at the T_{DM} given in Ga; the line representing a $^{176}Lu/^{177}Hf$ of 0.005 used to adjust for Pb loss in SRG-2 is indicated in light grey. CHUR - chondritic reservoir (bulk Earth). DM - depleted mantle; (Griffin et al.). Det - detrital. volcs - volcanics. (a) Indian subcontinent. (b) Kalahari craton. MNK - Murchison-Northern Kaapvaal. BN - Barberton north. GAB - Gaborone granite suite. NK-SMZ - Northern Kaapvaal, southern marginal zone. LIM - Limpopo belt. BS - Barberton south. FRAN - Franciscan arc. (c) China, Australia and Antarctica. JH - Jack Hills. (d) North Atlantic region and Baltica. Green - Greenland.

Figure 1 - colour for online only
Click here to download high resolution image

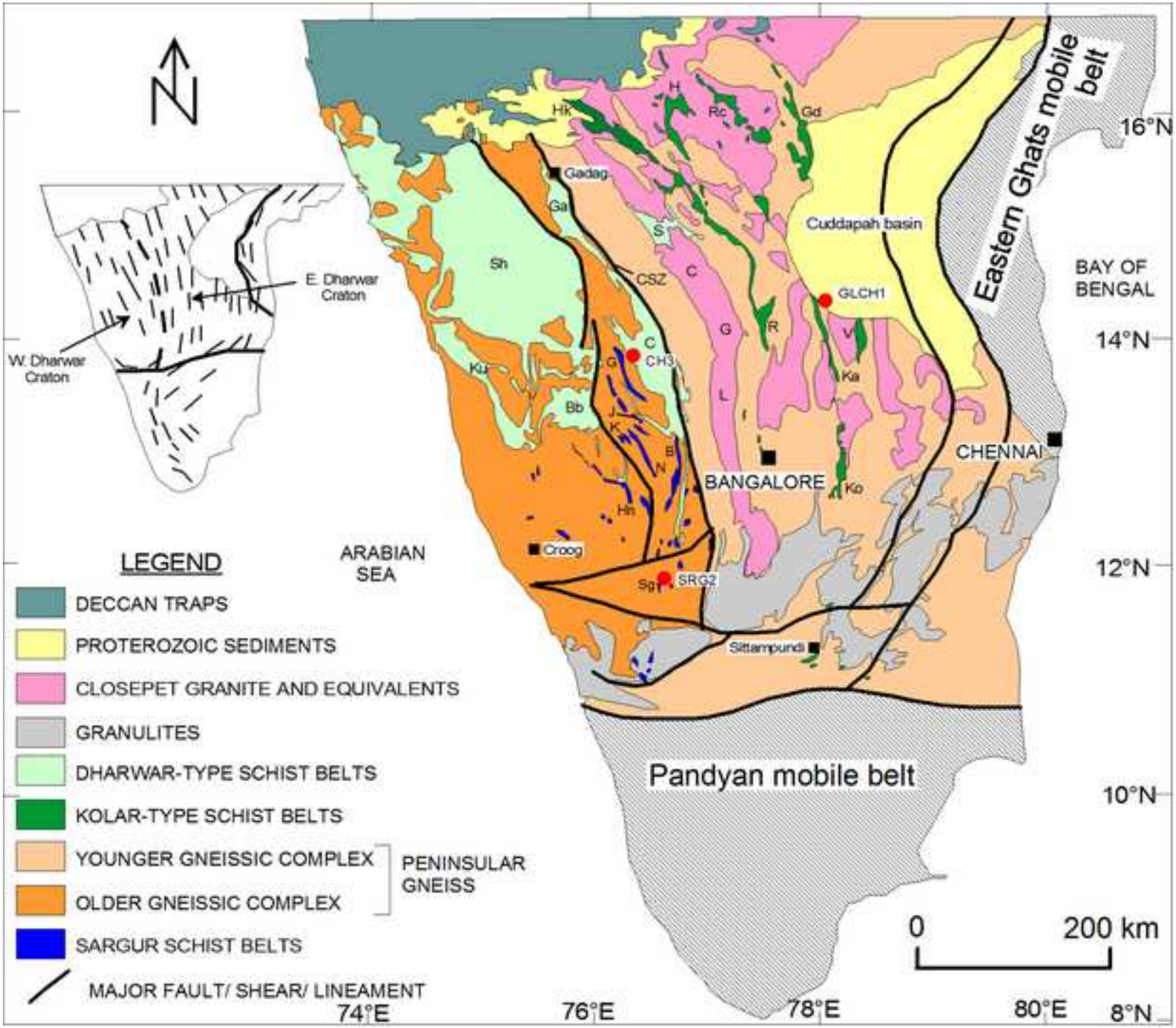

Figure 1 - B&W for print only

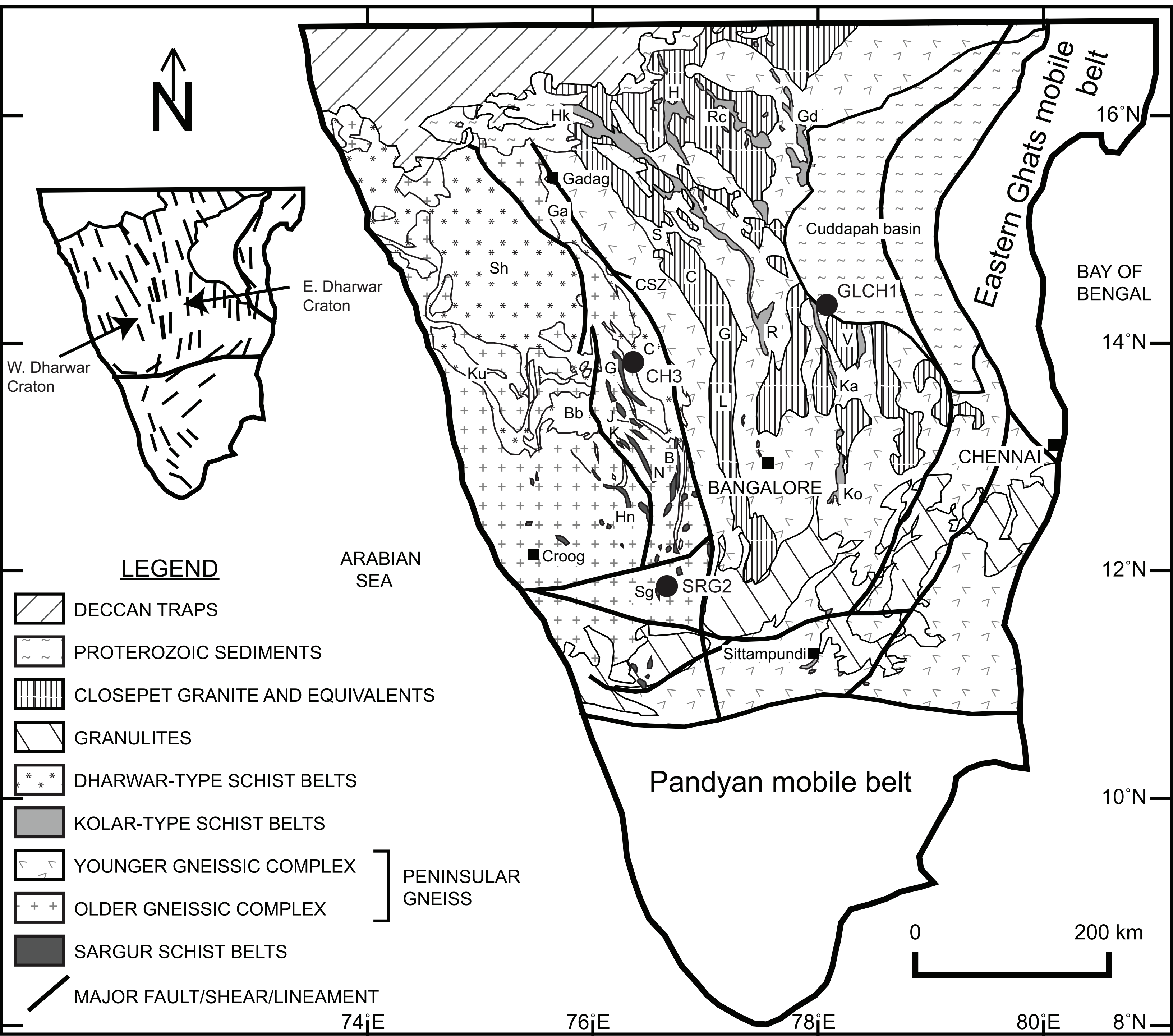

Figure 2

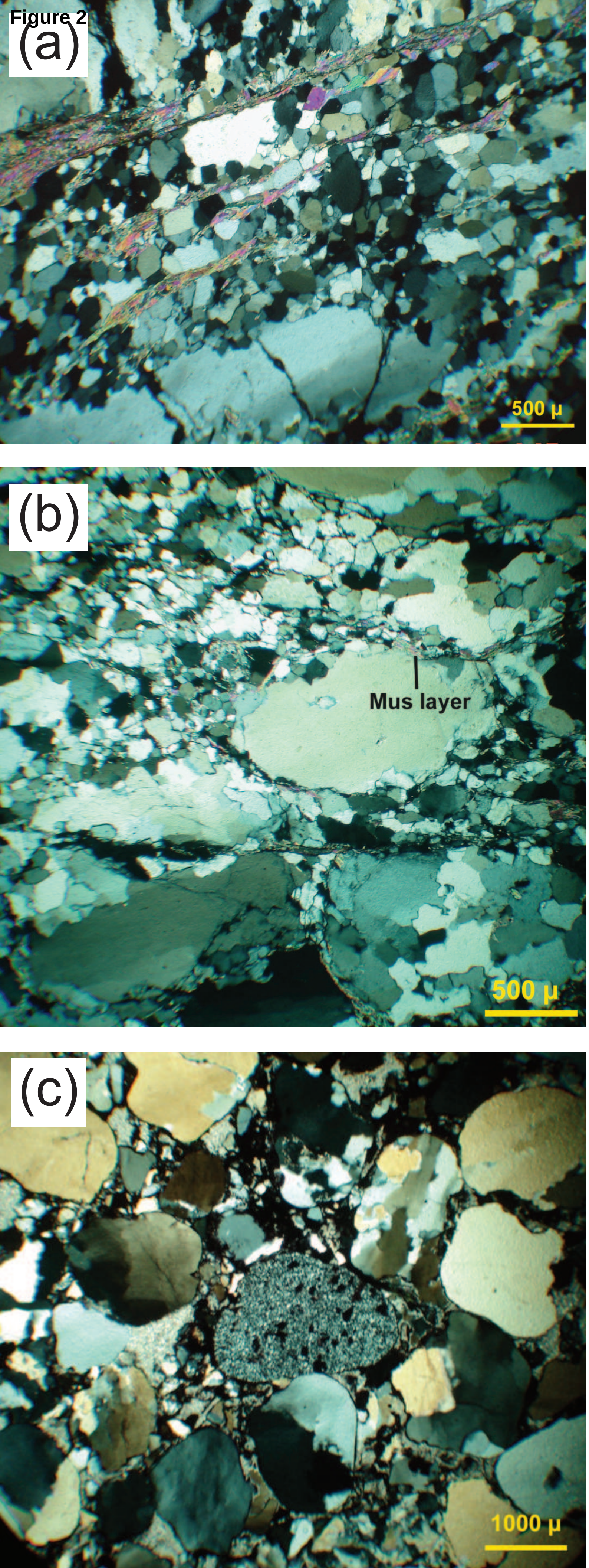

Figure 3

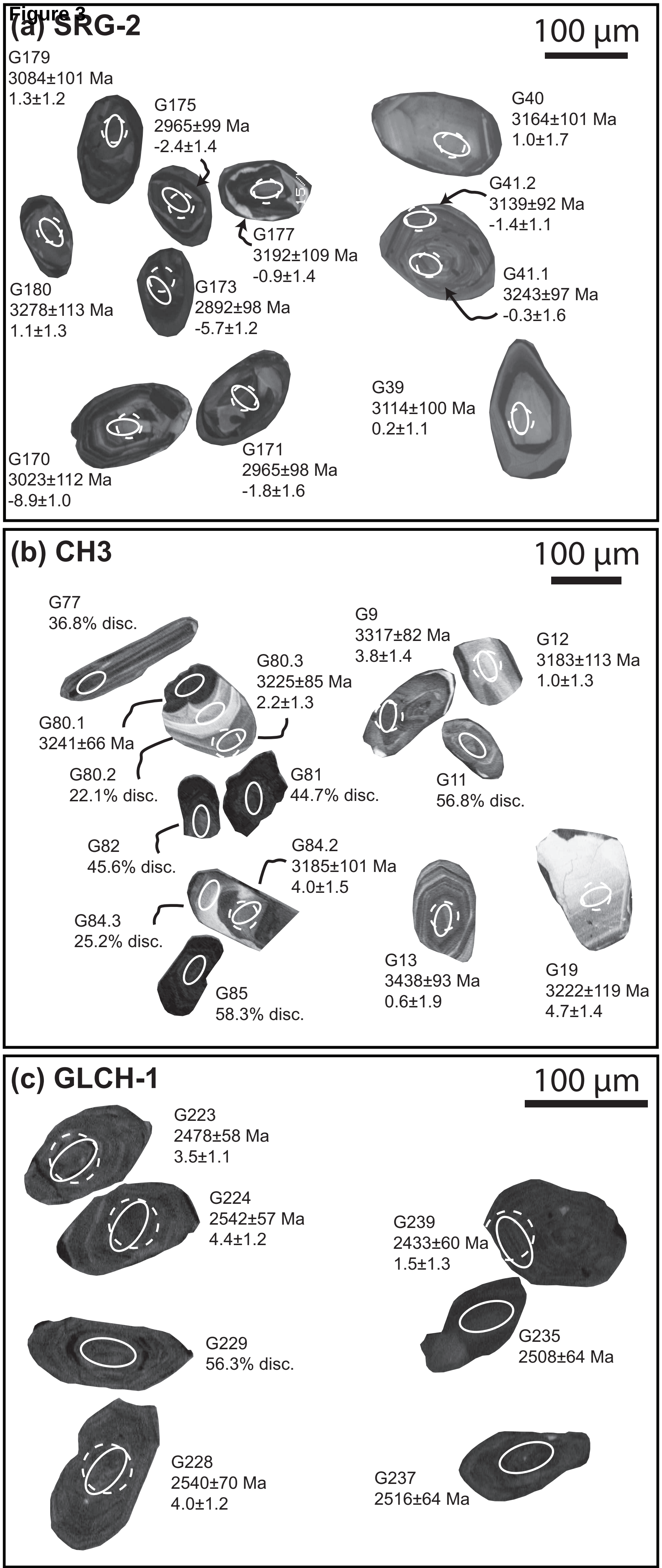

(a) SRG-2
100 µm
G179
3084±101 Ma
1.3±1.2
G175
2965±99 Ma
-2.4±1.4
G40
3164±101 Ma
1.0±1.7
G41.2
3139±92 Ma
-1.4±1.1
G177
3192±109 Ma
-0.9±1.4
G180
3278±113 Ma
1.1±1.3
G173
2892±98 Ma
-5.7±1.2
G41.1
3243±97 Ma
-0.3±1.6
G39
3114±100 Ma
0.2±1.1
G170
3023±112 Ma
-8.9±1.0
G171
2965±98 Ma
-1.8±1.6
(b) CH3
100 µm
G77
36.8% disc.
G9
3317±82 Ma
3.8±1.4
G12
3183±113 Ma
1.0±1.3
G80.3
3225±85 Ma
2.2±1.3
G80.1
3241±66 Ma
G80.2
22.1% disc.
G81
44.7% disc.
G11
56.8% disc.
G82
45.6% disc.
G84.2
3185±101 Ma
4.0±1.5
G84.3
25.2% disc.
G13
3438±93 Ma
0.6±1.9
G19
3222±119 Ma
4.7±1.4
G85
58.3% disc.
(c) GLCH-1
100 µm
G223
2478±58 Ma
3.5±1.1
G224
2542±57 Ma
4.4±1.2
G239
2433±60 Ma
1.5±1.3
G235
2508±64 Ma
G229
56.3% disc.
G228
2540±70 Ma
4.0±1.2
G237
2516±64 Ma

Figure 4

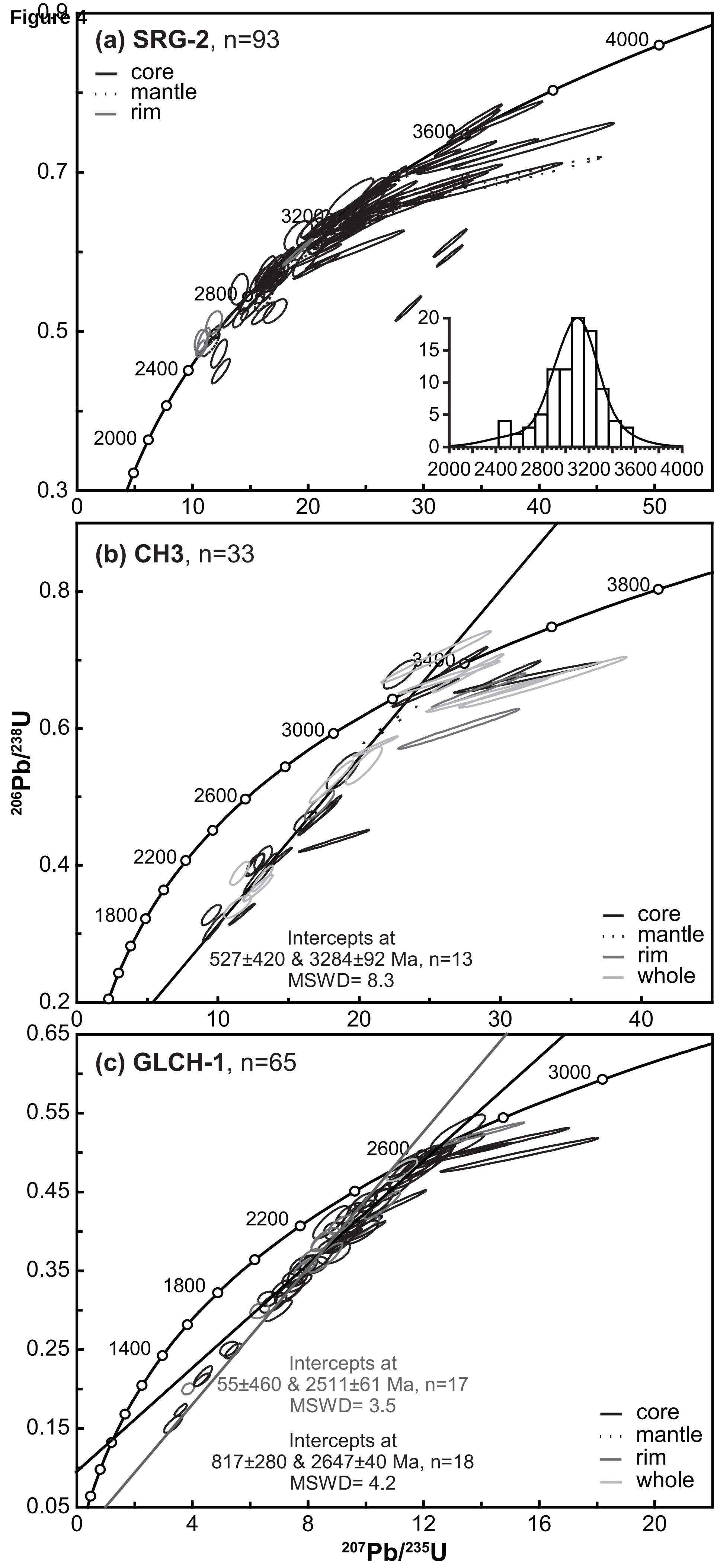

(a) SRG-2, n=93
core
mantle
rim
4000
3600
3200
2800
2400
2000
0.9
0.7
0.5
0.3
0
10
20
30
40
50
20
15
10
5
0
2000
2400
2800
3200
3600
4000
(b) CH3, n=33
3800
3400
3000
2600
2200
1800
0.8
0.6
0.4
0.2
Intercepts at
527±420 & 3284±92 Ma, n=13
MSWD= 8.3
core
mantle
rim
whole
(c) GLCH-1, n=65
3000
2600
2200
1800
1400
0.65
0.55
0.45
0.35
0.25
0.15
0.05
Intercepts at
55±460 & 2511±61 Ma, n=17
MSWD= 3.5
Intercepts at
817±280 & 2647±40 Ma, n=18
MSWD= 4.2
core
mantle
rim
whole
0
4
8
12
16
20
$^{206}Pb/^{238}U$
$^{207}Pb/^{235}U$

Figure 5

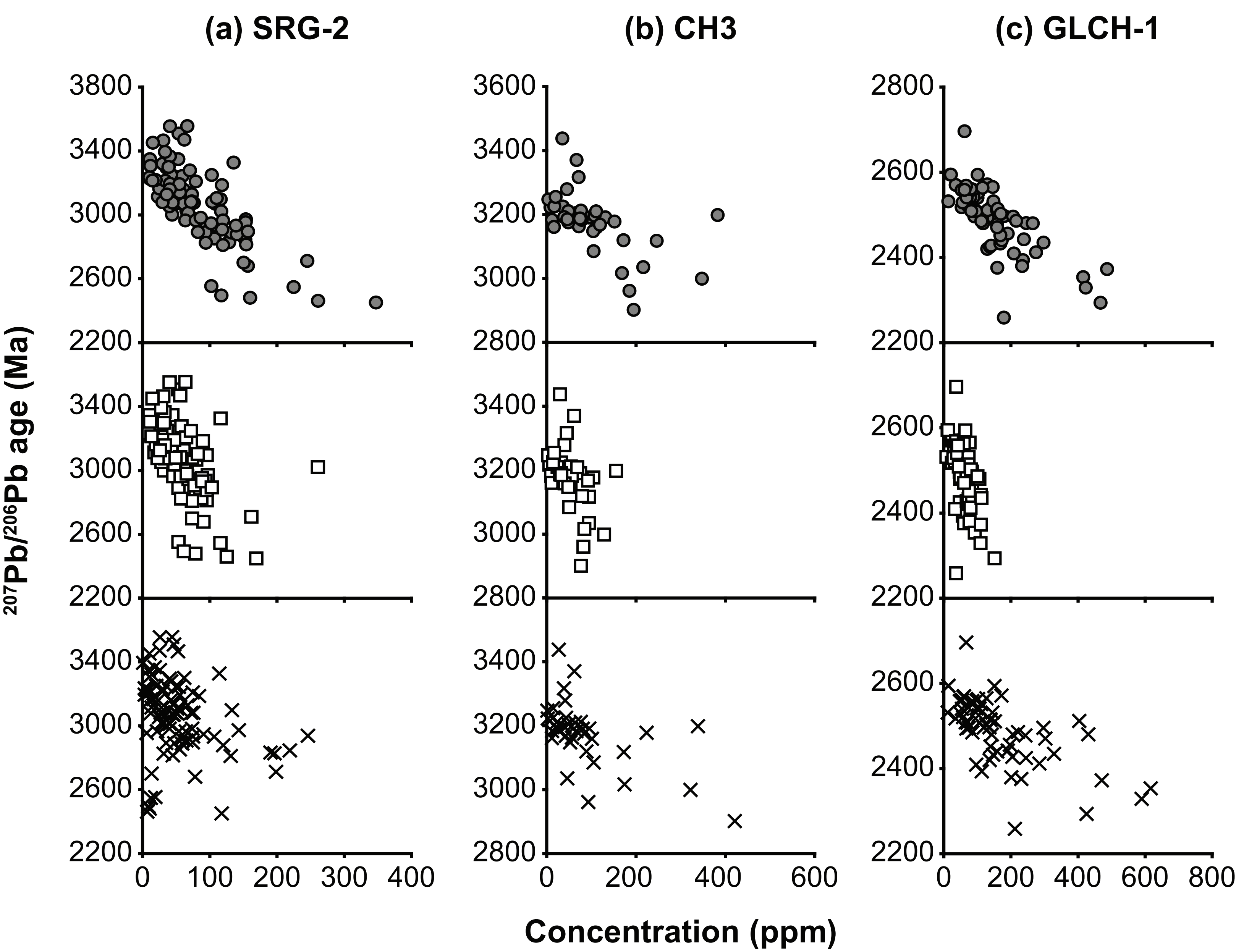

(a) SRG-2
(b) CH3
(c) GLCH-1
^{207}Pb/^{206}Pb age (Ma)
Concentration (ppm)
3800
3400
3000
2600
2200
3600
3200
2800
2400
0
100
200
300
400
600
800

Figure 6

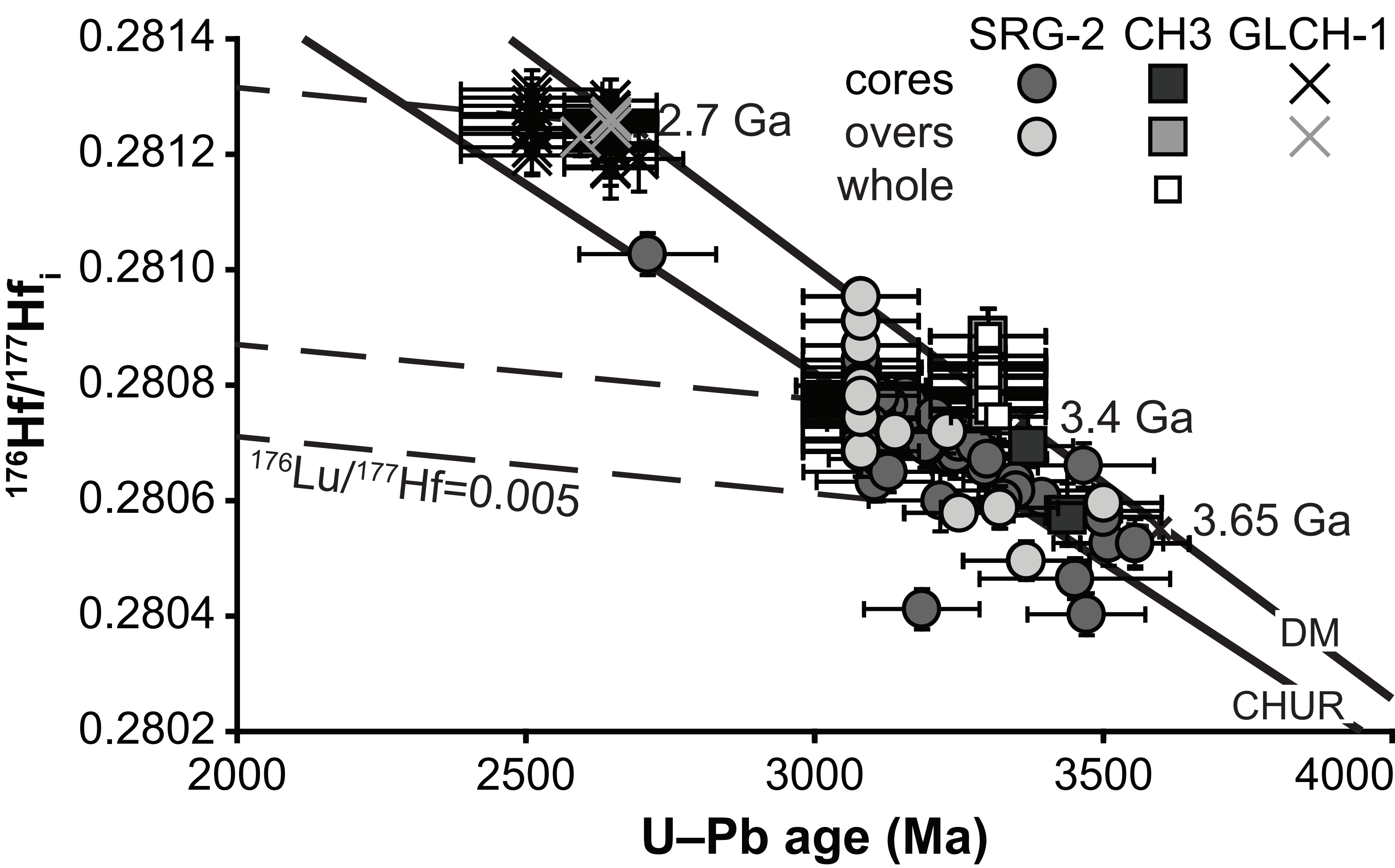

SRG-2
CH3
GLCH-1
cores
overs
whole
2.7 Ga
3.4 Ga
3.65 Ga
DM
CHUR
^{176}Lu/^{177}Hf=0.005
^{176}Hf/^{177}Hf$_i$
U–Pb age (Ma)
0.2814
0.2812
0.2810
0.2808
0.2806
0.2804
0.2802
2000
2500
3000
3500
4000

Figure 7

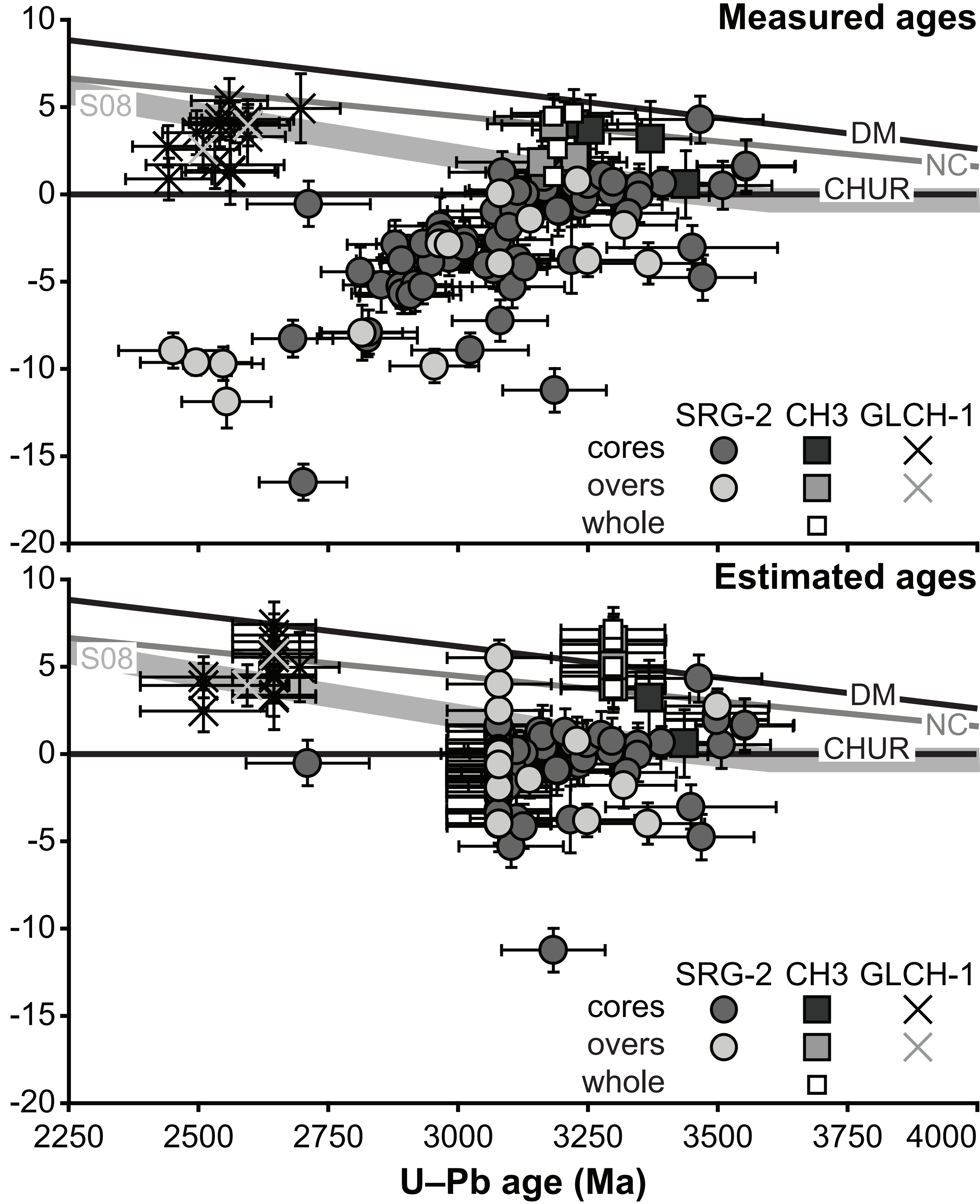

Measured ages
Estimated ages
εHf
U–Pb age (Ma)
DM
NC
CHUR
S08
SRG-2
CH3
GLCH-1
cores
overs
whole
10
5
0
-5
-10
-15
-20
2250
2500
2750
3000
3250
3500
3750
4000

Figure 8

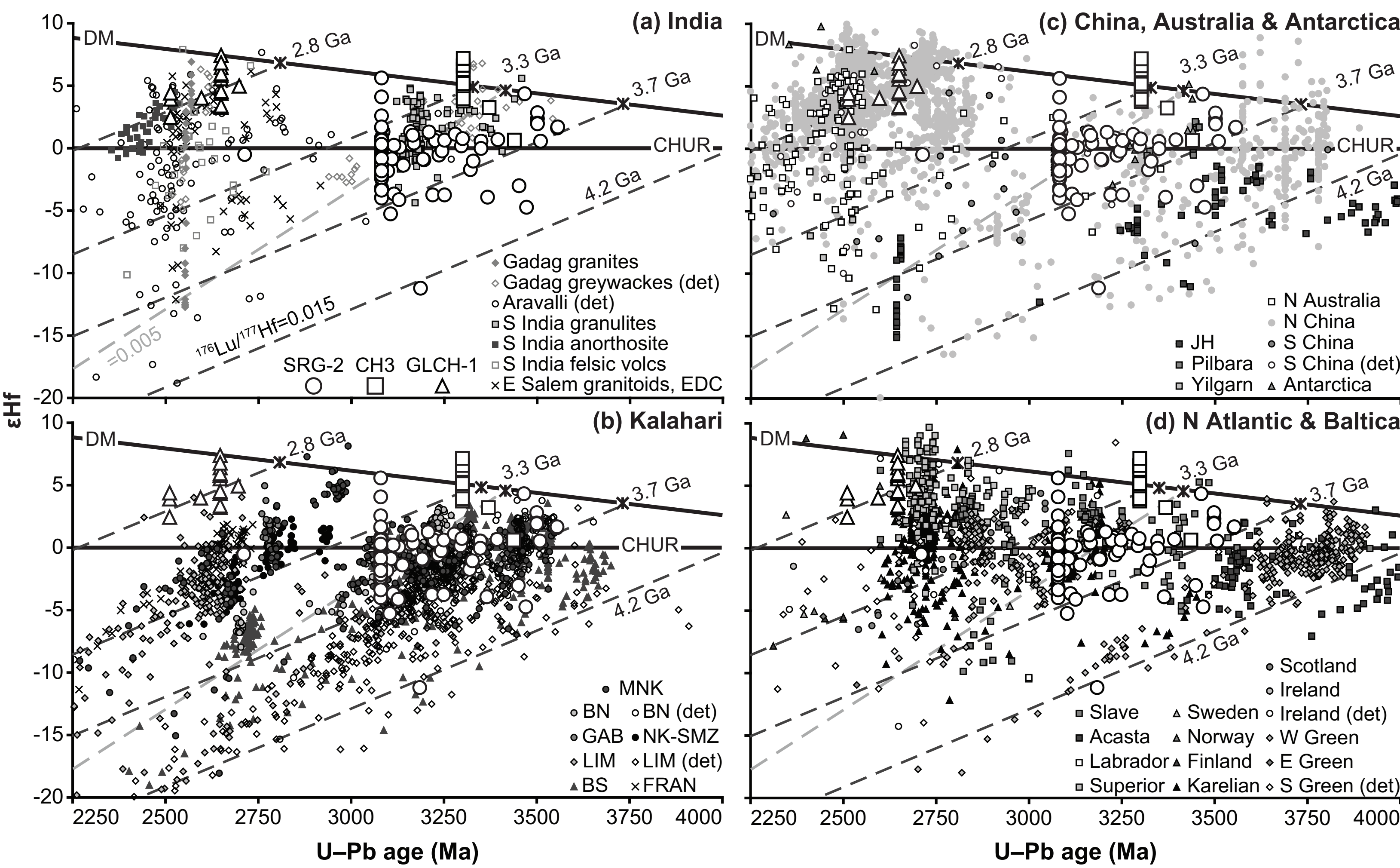
(a) India
(b) Kalahari
(c) China, Australia & Antarctica
(d) N Atlantic & Baltica
DM
CHUR
2.8 Ga
3.3 Ga
3.7 Ga
4.2 Ga
^{176}Lu/^{177}Hf=0.015
=0.005
Gadag granites
Gadag greywackes (det)
Aravalli (det)
S India granulites
S India anorthosite
S India felsic volcs
E Salem granitoids, EDC
SRG-2
CH3
GLCH-1
MNK
BN
BN (det)
GAB
NK-SMZ
LIM
LIM (det)
BS
FRAN
N Australia
N China
JH
S China
Pilbara
S China (det)
Yilgarn
Antarctica
Scotland
Ireland
Slave
Sweden
Ireland (det)
Acasta
Norway
W Green
Labrador
Finland
E Green
Superior
Karelian
S Green (det)
εHf
U–Pb age (Ma)

Table 1

Table 1

Simplified Precambrian stratigraphy of the Dharwar craton. The sampled horizons are marked in red.

Western Dharwar Craton (WDC)		**Eastern Dharwar Craton (EDC)**
Badami Group (0.6 Ga?)	**Kaladgi Supergroup**	**Kurnool Group, Bhima Group** (0.6 Ga?)
-------- *Unconformity* ---------	(~Cuddapah Supergroup)	-------- *Unconformity* ---------
Bagalkot Group		**Cuddapah Supergroup** (1.9-1.4 Ga?)
-------- *Unconformity* ---------		-------- *Unconformity* ---------
Younger granitoids (~2.6 Ga)		
Chitradurga Group	**Dharwar Supergroup**	**TTG gneisses, granites** (2.7-2.5 Ga)
(polymictic conglomerate,	(2.9-2.6 Ga)	**Kolar Group** (~2.7 Ga)
quartzite, greywacke,		(basalt, komatiite, chert,
pelite, BIF, basalt)		BIF, pelite, felsic volcanics)
Bababudan Group		
(oligomictic conglomerate,		
quartzite, basalt, BIF)		
-------- *Unconformity* ---------		
Sargur Group	**Granitic Gneisses**	
(3.3-3.0 Ga?)	(3.35-3.0 Ga)	-------------------
(quartzite, pelite, calc-		**Vestiges of older Gneisses** (~ 3.3-3.1 Ga)
silicate, basalt, koma-		and **supracrustals** (~ 3.3 Ga?)
tiite, BIF, layered mafic-		
ultramafics)		

***Highlights (for review)**

- Terrane accumulation in the Dharwar craton began ~3 Ga in older Western block
- Final cratonisation at 2.5 Ga is much later than other Archaean cratons
- Tectonic, not genetic, links with the Kaapvaal and north China cratons